



ALMA MATER STUDIORUM  
UNIVERSITÀ DI BOLOGNA

**DOTTORATO DI RICERCA IN  
SCIENZE CHIRURGICHE**

Ciclo 36

**Settore Concorsuale:** 06/E3 - NEUROCHIRURGIA E CHIRURGIA MAXILLO FACCIALE

**Settore Scientifico Disciplinare:** MED/29 CHIRURGIA MAXILLO FACCIALE

**APPLICATION OF AUGMENTED REALITY IN CRANIOFACIAL  
SURGERY: A FEASIBILITY STUDY**

**Presentata da:** Federica Ruggiero

**Coordinatore Dottorato**

Bianca Maria Piraccini

**Supervisore**

Achille Tarsitano

**Co-supervisor**

Emanuela Marcelli- Laura Cercenelli

**Esame finale anno 2024**

# Table of Contents

<b>ABSTRACT</b>	6
<b>CHAPTER 1 INTRODUCTION</b>	
1.1 Research Introduction	9
1.2 Background	10
1.2.1 Augmented Reality	10
1.2.2 HoloLens2	14
1.2.3 Craniofacial surgery	16
1.2.3.1. Craniosynostosis	16
1.3 Objective and aims	25
<b>CHAPTER 2 OBJECTIVE 1: FRONTO-ORBITAL REMODELLING: TECHNIQUE OF CHOICE</b>	
2.1 Introduction	27
2.2 Methodology	29
2.2.1 Patient population	29
2.2.2 Surgical techniques	30
2.2.3. Image acquisition	33
2.2.4. Cephalometric measurements	34
2.3 Results	35
2.3.1. Cephalometric measurements	35
2.3.2. Clinical Outcomes	38
2.4 Discussion	38

## **CHAPTER 3 OBJECTIVE 2: PRECLINICAL APPLICATION OF HOLOLENS2**

3.1 Rationale of the Survey	40
3.2 Materials and methods	43
3.2.1 Methodology	43
3.2.2 Development Phase	43
3.2.3 Experimental Phase.	47
3.2.4 Statistical Analysis	49
3.3 Results	49
3.4 Discussion	52
3.5 Conclusions	54

## **CHAPTER 4 OBJECTIVE 3 APPLICATION OF HOLOLENS2 IN A CLINICAL SETTING**

4.1 Rationale of the Survey	57
4.2 Materials and methods	57
4.2.1 Development Phase	58
4.2.1.1. Virtual Content Preparation	58
4.2.1.2. 3D Printing of CAD/CAM Cutting-Guides for Testing Accuracy	58
4.2.1.3. The AR Application	59
4.2.1.4. Image target tracking	61
4.2.1.5. Experimental Phase	61
4.2.2 Statistical Analysis	63

4.3 Results	64
4.3.1. Single Patient Analysis	68

4.4 Discussion

## **CHAPTER 5 USERS' EXPERIENCE**

5.1 Users' Experience	74
5.2 Users' Experience: results	73
5.3 Discussion	77

## **CHAPTER 6 CONCLUSIONS**

6.1 Conclusions	80
-----------------	----

<b>REFERENCES</b>	81
-------------------	----

## **ACKNOWLEDGEMENTS**



# ABSTRACT

**Purpose**—Augmented Reality (AR) is a novel promising technology, which is gaining increasing success in the medical field. A number of applications in surgery have been described, but few studies have been focusing on pediatric craniofacial surgery. In this comprehensive research project, the Authors have been implementing a system for intraoperative surgical navigation by means of HoloLens 2 by Microsoft, applied to pediatric craniofacial surgery. The Authors tested the device in a preclinical setting first, and then moved to real patients.

**Methods**— the Authors assessed the accuracy of the HoloLens 2 by performing 36 procedures in vitro on a printed 3D model of a patient. When applied in reality, 10 patients were prospectively enrolled in the study. The virtual surgical planning was designed for each patient and uploaded onto the software which allows for the AR interface and the standard neurosurgical navigator. For each patient, the surgeon has been drawing osteotomy lines both under the guidance of HoloLens2 and of the neurosurgical navigator. The Author then checked the accuracy by means of calibrated CAD CAM cutting guides with different grooves, in order to assess the accuracy of the osteotomies performed. We tested levels of accuracy of  $\pm 1.5$  mm and  $\pm 1$  mm .

**Results**—in the preclinical setting, the HoloLens 2 performed with levels of accuracy of 1.5 mm, whereas in the real setting, surgeons were able to trace the osteotomy lines under the AR guidance for an amount of 45% (0.4 SD) of the entire line, with an accuracy level of  $\pm 1.5$  mm. This percentage lowers to 34% (0.4 SD) when assessing accuracy level of  $\pm 1$  mm. The results of the same tasks for the standard navigator are 36% and 16%, for  $\pm 1.5$  mm and  $\pm 1$  mm accuracy level, respectively.

**Conclusions** – The HoloLens2 did not perform worse than the standard navigator and performed even better with an accuracy level of  $\pm 1$  mm. The Authors reported encouraging results both in the preclinical and the clinical setting. We recognize that we have strong limitations, especially related to the small cohort of patients.

# Chapter 1 INTRODUCTION

## **Chapter 1: Introduction**

### **1.1 Research introduction**

Craniofacial surgery addresses a spectrum of congenital and acquired cranial and facial anomalies [1]. The discipline demands surgical precision, and a deep knowledge of the anatomy to restore both function and form. Augmented reality (AR), as exemplified by the HoloLens, has emerged as a transformative technology, gaining more and more success in the medical environment [2].

In this doctoral thesis the Authors investigate the feasibility of AR through head mounted display (HMD) such as HoloLens 2 (Microsoft), applied to pediatric craniofacial surgery, uncovering challenges, and advances born of their integration. Through a stepped study, we want to assess the feasibility of this technology in the field of craniofacial surgery.

Microsoft's HoloLens technology represents a pioneering stride in augmented reality, immersing surgeons in a holographically enriched surgical environment [3]. In the sphere of craniofacial surgery, it can offer real-time anatomical overlays, dynamic visualizations, and precision-guided interventions.

The Authors structured the research in three main objectives, each of them implicating the following.

We started from studying the best technique for fronto-orbital remodeling (FOR) (a surgical technique to address forehead dysmorphologies in toddlers) and then use it to test the HoloLens2 preclinically.

From the encouraging results obtained, the Authors started applying the technology on actual patients and on several craniofacial procedures.

In summation, AR might redefine surgical navigation in profound ways [4]. Their appliances are still debated, but further studies might lead to a proper integration of this promising technology into the operating theatres.

## **1.2. Background**

### **1.2.1. Augmented reality**

Augmented Reality (AR), often abbreviated as AR, is a promising technology which allows the user to experience a full integration between real environment and virtual information [5]. This stands in stark contrast to its immersive counterpart, Virtual Reality (VR), which immerses users entirely within synthetic digital landscapes. In AR, the real world is augmented, enriched, and layered with virtual elements [5,6].

Azuma's description of AR includes these characteristics [6]. AR serves as a conduit that connects the tangible physical world with the digital domain, fostering a dynamic integration between reality and the virtual.

In the medical field, AR emerges as a transformative tool, driven by the need to visualize intricate medical data within the same physical space as the patient [7]. Four key domains of potential enhancement come to the fore:

1. **Image Fusion**: Augmented Reality's capacity to blend the real world with one or multiple images streamlines focus, obviating the need for users to shift their attention between the physical world and a screen. [8]
2. **3D Interaction**: Augmented Reality relies on the interaction of the users with virtual three-dimensional objects
3. **3D Visualization**: AR's stereoscopic viewing significantly enhances spatial object perception compared to conventional 2D displays.
4. **Hand-eye Coordination**: Augmented Reality's unique attribute of allowing users to observe their actual hand interacting with the virtual world eliminates the need for mental mapping between displayed objects and their real-world counterparts.

Augmented Reality predominantly takes the form of a head-mounted display (HMD), akin to a helmet or glasses worn by the user, incorporating individual displays in front of each eye to facilitate stereoscopic imaging and intensify the perception of depth [9,10].

HMDs confront a distinct challenge—simultaneously presenting the real world to the user. This challenge is met through two primary methods. Firstly, optical see-through HMDs replicate the transparency of conventional glasses, enabling users to perceive the physical environment directly. Alternatively, video see-through HMDs employ onboard cameras to capture the real world, digitally

superimposing it onto the user's view, achieving a seamless fusion of the real and virtual information [8,11]

Augmented Reality falls within the broader context of Mixed Reality, a concept articulated by Milgram et al. [12]. Within this framework, they establish a reality-virtuality continuum encompassing all manifestations of Mixed Reality.

Augmented Reality and its counterpart, Virtual Reality, find their distinctive positions along this spectrum. Augmented Reality involves augmenting the real world with virtual elements, whereas Virtual reality, immerses users primarily in a virtual world, supplemented by real-world objects.

Crucially, the continuum underscores that the transition from Augmented Reality to Augmented Virtuality is gradual, devoid of clear demarcation points, as various mixed reality experiences fluidly merge the realms of reality and the virtual [12].

As AR technology stands on the concept of "onlay," where the camera captures the object within its frame, the system recognizes it, and a new layer of interaction unfolds, overlaying and seamlessly integrating virtual information with the real-world object being framed [13].

The application of AR extends its reach into various fields, notably within the surgical navigation [13-29]. In the medical context, AR takes the real environment and projects a virtual layer upon it, custom-tailored to each patient's unique anatomy [13-29].

AR technology is also classified into two main categories: immersive and non-immersive [5]. In the former, the operator feels fully integrated into the surrounding reality, while in the latter, a computer orchestrates the integration of diverse levels of information.

Today, surgical navigation heavily relies on established AR technology, facilitating procedures like ventriculo-peritoneal shunt insertion and craniofacial and neurosurgical tumor resections, which are now routinely conducted with the aid of navigation systems [18]. Traditional surgical navigation involves external devices that track the patient's position and merge information from CT scans or MRI onto a screen.

However, conventional navigation comes with its own set of limitations, including the constant need for the operator to shift their focus between the patient and the screen [8,13].

AR headsets, such as Microsoft's HoloLens, represent a technological leap that overcomes this limitation, offering a comprehensive navigation experience. These headsets feature integrated displays that allow surgeons to access pertinent information while keeping their attention on the surgical field [13]. They enable the visualization of critical anatomical structures, trajectories for osteotomies, and incision points without compromising the surgeon's natural field of vision, as the lenses remain clear.

### **1.2.2. HoloLens 2**

Among the AR devices that have gained prominence in healthcare, Microsoft's HoloLens 2 stands out. This wearable AR headset offers the ability to superimpose holographic virtual objects onto the real-world environment, enabling medical professionals to visualize, interact with, and manipulate digital information.

The HoloLens 2 represent the second generation of mixed reality headsets. The device is equipped with a high-resolution visor that enables the projection of three-dimensional holographic images onto the user's field of view and an in-built camera.

In the context of medicine, HoloLens 2 has gained recognition for its potential to transform medical training, surgical planning, intraoperative guidance, and patient education.

Medical education has witnessed a paradigm shift with the introduction of HoloLens 2. It offers a unique platform for immersive learning experiences, enabling medical students and professionals to visualize anatomical structures in three dimensions. For example, the device can render detailed holographic representations of the human body, allowing students to dissect virtual cadavers, explore complex organ systems, and understand pathological conditions in a realistic and interactive manner [30].

HoloLens 2 has been recently gaining more recognition in the surgical field. Surgeons can use the device to overlay patient-specific medical imaging data, such as CT scans or MRI images, onto the surgical field in real-time. This

augmented view aids in navigation, enabling surgeons to locate critical structures, plan optimal incisions, and perform complex procedures with greater confidence [31]. Additionally, the device supports telemedicine applications by allowing remote experts to provide guidance during surgery, potentially improving outcomes in challenging cases [32].

Physicians can also use the device to visualize and explain medical conditions to patients and their families in an understandable and engaging manner. For example, it can display 3D models of tumors or treatment options, enabling patients to make informed choices about their care plans [33].

In conclusion, the HoloLens 2 represent a significant technological advancement with transformative potential in the field of medicine. Its applications in medical education, surgical procedures, and patient-centered care might be a solid possibility in the future. As further research and development continue, the integration of HoloLens 2 and similar AR devices is likely to become more widespread, offering innovative solutions to complex challenges in healthcare.

### **1.2.3. Craniofacial Surgery**

Craniofacial surgery stands as a subspecialty dedicated to addressing both congenital and acquired deformities encompassing the head, skull, face, neck, jaws, and their related anatomical structures. [34,35].

Craniofacial Surgery addresses a broad spectrum of defects, including but not limited to craniosynostosis (both isolated and syndromic variations), exceptionally rare craniofacial clefts etc.

### **1.2.3.1 Craniosynostosis**

The human skull consists of interconnected bones joined together by cranial sutures. Typically, these sutures gradually fuse during the initial years after birth. However, in infants where one or more sutures fuse prematurely, it hinders the natural expansion of the skull. This, in turn, triggers compensatory mechanisms that lead to irregular patterns of growth. Notably, skull growth occurs perpendicular to these sutures. Thus, when a suture fuses too early, growth along the axis defined by that suture becomes restricted, while growth near the remaining sutures becomes accelerated, resulting in an atypical head shape, as per Virchow's theory [36].

The primary driving force behind the rapid skull growth observed in the early years of life is the expanding brain. Any impediment to the growth potential of the skull can constrain the space required by the growing brain. In instances where compensatory mechanisms fail to provide sufficient room for the enlarging brain, craniosynostosis can manifest, accompanied by elevated intracranial pressure [37].

Craniosynostosis is classified as "simple" when only one suture is involved and "complex" when two or more sutures are affected. It can occur either as part of a broader syndrome or as an isolated defect, referred to as "nonsyndromic" [38]. (see figure 1)



**Figure 1:** top left and right, an example of sagittal synostosis, giving the scaphocephalic shape; bottom left and right: metopic synostosis, giving trigonocephalic shape (please refer to the text for further explanations)

### **Scaphocephaly**

Scaphocephaly is characterized by the premature fusion of the sagittal suture, which extends from the front to the back of the head. This condition results in a distinctive head shape resembling a long, narrow boat, hence the term "scapho" (figure 1, top). To compensate for the limited growth along the sagittal

suture, the head exhibits compensatory growth patterns, particularly forward at the coronal suture. This compensatory growth leads to the development of a prominent forehead, frontal bossing, and an accentuated posterior head shape known as "coning" [39].

### **Trigonocephaly**

The premature fusion of the metopic suture, which ranks as the second most prevalent form of single-suture craniosynostosis, is observed in approximately 1 in 7,000 to 1 in 15,000 newborns [40]. This condition typically results in the classic trigonocephalic phenotype [41,42]. Notably, there appears to be a stronger genetic correlation when compared to other forms of non-syndromic craniosynostosis, with a higher incidence among siblings and first-degree relatives [43-46] (figure 1).

Clinical presentations of metopic suture fusion exhibit a wide spectrum of severity. This spectrum ranges from the presence of a simple metopic ridge with a normal forehead shape to more severe cases characterized by narrowed foreheads, loss of the natural frontal curvature, supraorbital retrusion, hypotelorism, and various orbital anomalies such as raised eyebrows and epicanthus [40].

Historically, both morphological and functional criteria have been considered to establish universal surgery guidelines, albeit without achieving definitive outcomes. In terms of neurocognitive aspects, approximately 15% to 30% of children with trigonocephaly experience speech and language delays [47-

49]. However, most available studies do not demonstrate clear correlations between the severity of trigonocephalic deformities and impairment in neurocognitive development [50,51]. Moreover, there is limited evidence of significant variations in these aspects between patients who undergo surgical intervention and those treated conservatively [47]. Only three multicenter studies have reported lower motor and mental scores in children with isolated trigonocephaly [52-54] .

The estimated risk of intracranial hypertension in individuals with metopic suture fusion is approximately 9%, which is the lowest among all non-syndromic craniosynostosis cases [55].

### **Plagiocephaly**

It can be anterior or posterior.

#### **Anterior Plagiocephaly:**

Anterior plagiocephaly is determined by unilateral coronal synostosis [56]. Infants born with unilateral coronal synostosis develop a skewed head shape, referred to as plagiocephaly, due to compensatory mechanisms [56].

The sagittal suture divides the coronal suture into two halves. In unilateral coronal synostosis, either the right or left side of the coronal suture fuses with the sagittal suture, resulting in asymmetry [56]. This asymmetry is evident in the deformity of the skull, facial features, and associated complications [56].

Growth is halted in the plane perpendicular to the fused suture, leading to a flattened forehead, but only on the same side as the closed suture. Ipsilateral refers to the same side as the closed suture. Compensatory growth occurs both

in a parallel plane and a perpendicular plane. Parallel plane growth is observed at the metopic and sagittal sutures, resulting in bulging at the temporal fossa [56]. Perpendicular plane growth occurs on the side of the head with the open coronal suture, leading to forward bulging of half of the forehead.

Top view assessment of the skull reveals frontal bone asymmetry, increased skull width, and forward ear displacement on the ipsilateral side of the head [57]. Frontal view assessment shows facial asymmetry, including a chin point and tip of the nose deviation. The chin point shifts toward the contralateral side due to the ipsilateral forward displacement of the temporomandibular joint and ear. The tip of the nose also points toward the contralateral side [. Complications associated with skull deformity include jaw malocclusion in up to 90% of cases, mild strabismus due to uneven orbital placement, and refractive errors, particularly astigmatism, arising from uneven orbital development [58].

### **Posterior Plagiocephaly:**

Unilateral lambdoid synostosis, also known as posterior plagiocephaly, results in a skewed head shape similar to unilateral coronal synostosis. However, in this case, the deformity primarily affects the occiput.

According to Virchow's law, growth restriction occurs on the ipsilateral side of the head, with compensatory growth on the contralateral side. This growth pattern impacts the base of the skull, resulting in an uneven profile when viewed from behind. It also influences the cervical spine, which exhibits curvature [59].

Additionally, a bulging of the mastoid can be observed when viewed from behind, with minimal forehead asymmetries typically present [60].

### **Brachycephaly:**

Brachycephaly, commonly referred to as a "short head," arises from the closure of both coronal sutures.. According to Virchow's law, this condition leads to restricted growth both in the forward and backward directions, resulting in recessed frontal bones and a flattened occiput.. Compensatory growth occurs sideways due to the sagittal suture and upward due to the lambdoid sutures [60].

### **Turricephaly:**

Turricephaly, also known as oxycephaly, acrocephaly, or high-head syndrome, falls under the category of cephalic disorders. This term is sometimes used to describe premature closure of not only the coronal suture but also any other suture, such as the lambdoid suture.

### **Pansynostosis:**

It describes cases with three or more cranial sutures closed [61].

Pansynostosis can manifest in various ways. It may appear similar to primary microcephaly, characterized by a significantly small head with normal proportions [62]. The most severe form of pansynostosis is kleeblattschädel (cloverleaf skull), which results in bulging of different cranial vault bones [62].

## **Syndromic Craniosynostosis**

Syndromic craniosynostoses, which are genetically determined, constitute a diverse group of conditions primarily associated with gain-of-function mutations. These mutations frequently involve genes related to bone and cartilage development, notably the fibroblast growth factor receptor (FGFR) family (Crouzon, Apert, Pfeiffer Syndromes). While exceptions like craniofrontonasal dysplasia (CFND) with X-linked inheritance and Carpenter syndrome with autosomal recessive inheritance exist, the majority of these syndromes exhibit an autosomal dominant mode of inheritance [63, 64]. It's noteworthy that around half of the causative mutations occur spontaneously (de novo), often linked to advanced paternal age, suggesting potential genetic instability that accumulates over time [65]. In addition to craniofacial anomalies, these syndromes give rise to complex visceral and skeletal abnormalities, particularly affecting the hands and feet [66,67].

The overall incidence of craniosynostosis is estimated to range from 1 in 2,100 to 1 in 2,500 live births [68]. However, this incidence varies significantly depending on the specific suture(s) involved. Some of the most commonly diagnosed craniosynostosis-associated syndromes include Muenke (1 in 10,000–1 in 30,000), Crouzon (1 in 25,000), Pfeiffer (1 in 100,000), Apert (1 in 100,000), and Saethre-Chotzen (1 in 25,000–50,000) [Wilkie et al., 2017]. With the exception of Saethre-Chotzen syndrome (SCS), which results from a loss-of-function mutation in the TWIST gene [69], these syndromes are characterized by gain-of-function mutations in the FGFR gene. We also remember less common syndromes, such as CFND and the more recently identified syndromes caused by ERF and TCF12 mutations.

Given the varied clinical presentation of these conditions, a multidisciplinary approach is imperative when caring for affected children and their families. [70]

The dissertation of each single syndrome, is out of the intentions of this work, please refer to the summary table 1 following, courtesy of O'Hara, Ruggiero et al. [70]

Syndrome	Raised ICP	Airway compromise	Exorbitism	Midface hypoplasia	Hyper-telorism	Operative intervention	Hand involvement	Other features
Apert	++	++	++ Class III	+++	++	PVE then bipartition or LFII/III	+++	Cleft, OSA, strabismus, developmental delay
Crouzon	++	++	++ Class III	++/+	-	PVE +/- monobloc	-	Cervical vertebral fusion
Pfeiffer	+++	+++	+++ Class III	+++	+/-	PVE +/- early monobloc	Broad deviated thumbs and toes	Multi-level airway anomalies, Chiari, spinal anomalies
Muenke	+	-	-	-	-	PVE +/- FOR	-	Hearing loss, seizures
Saethre-Chotzen	+	-	+/- Often class III	+/-	-	PVE +/- FOR, FOR, rarely midface	+/-mild	Ptosis, strabismus, ear anomaly
CFND	-	-	-	-	+++	Hypertelorism correction +/- FOR +/- PVE	-	Wiry hair, nail anomalies, strabismus, cleft, CNS anomalies
TCF12	+/-	-	-	-	-	PVE +/- FOR, FOR	-	Severe turribrachycephaly
ERF	++	-	+ Class III	+	+	Late vault expansion	-	Behavioural issues, hearing loss, Chiari, language delays

CFND, craniofrontonasal dysplasia; FOR, fronto-orbital remodelling; ICP, intracranial pressure; LF, Le Fort fracture; OSA, obstructive sleep apnea; PVE, posterior vault expansion. +, mild; ++, moderate; +++, severe; -, not present; +/-, sporadically.

**Table 1:** summary of the characteristics of the most common syndromic craniosynostosis

#### **1.2.4 Objective and aims**

**Objective 1: indicate a fronto-orbital remodelling technique of choice in between the ones adopted in our Centre, to start testing the AR by means of HoloLens 2**

**Objective 2: assess the feasibility of HoloLens 2 in craniofacial surgery in an experimental preclinical setting and implement the navigation system**

**Objective 3: apply the intraoperative navigation system by means of HoloLens 2 on simple surgical tasks in real patients.**

Once we have indicated the technique of choice, we have used it to test HoloLens2 in a preclinical experimental setting.

In controlled experimental instances, we found a good reliability of the device and we have obtained the approval for the use on actual patients.

We want to assess if AR might have a future as a true support in craniofacial surgery.

# Chapter 2 OBJECTIVE 1

**FRONT-ORIBITAL REMODELLING:**

**TECHNIQUE OF CHOICE**

Metopic synostosis is a congenital dysmorphology causing the premature fusion of the metopic suture. This accounts for the peculiar head-shape that these children present and known as trigonocephaly.

Each center addresses it in their own technique, but no general consensus has been reached. Furthermore, few studies report quantitative evaluations of the correction obtained: hence, it is mostly based on the experience of the surgeon.

In this study, the Authors have been first reviewing their case series, and then indicated their technique of choice in order to test it with AR in a preclinical setting.

## **2.1 Introduction**

Craniosynostosis is a relatively common birth deformity, occurring in approximately 1 in 2500 live births. Among these cases, nonsyndromic forms, which do not involve associated syndromes, constitute the majority, accounting for around three-quarters of all craniosynostosis cases. Specifically, the premature fusion of the metopic suture, the second most common form of single-suture craniosynostosis, is reported to occur in newborns at a frequency ranging between 1 in 7000 and 1 in 15000. This condition typically manifests as the classic trigonocephalic phenotype [42, 55].

Metopic synostosis exhibits a stronger genetic correlation when compared to other forms of nonsyndromic craniosynostosis, with a higher prevalence among siblings and first-degree relatives. Clinical presentations of metopic synostosis vary widely in severity, ranging from cases characterized by a simple metopic ridge and a normal forehead shape to severe presentations with marked

narrowing of the forehead, loss of the natural frontal curvature, supraorbital retrusion, hypotelorism, and other orbital anomalies such as upward eyebrows, epicanthus, and strabismus. [50]

In terms of neurocognitive aspects, approximately 15% to 30% of children with trigonocephaly report speech and language delays. However, most available studies have failed to demonstrate a clear correlation between the severity of trigonocephalic shape and impaired neurocognitive development, nor have they shown significant variations in these aspects between patients who underwent surgery and those managed conservatively [53,54,56]. Additionally, the estimated risk of intracranial hypertension in metopic synostosis is relatively low, standing at 9%, which is the lowest among all nonsyndromic craniosynostosis cases. 54

Therefore, the indications for treatment in metopic synostosis remain a subject of debate, considering factors like the risk of increased intracranial pressure (ICP) and cosmetic concerns. Several reports have attempted to identify universal criteria for grading the severity of trigonocephaly, including measures like forehead curvature, interfrontal angle, and intercanthal distance.

In the center of the Pediatric Neurosurgery Unit of the IRCCS Istituto delle Neuroscienze di Bologna ISNB, we have primarily employed two distinct surgical techniques for treating children with metopic synostosis, ranging from mild to severe cases, over time. The objective of this study is to conduct a comparative analysis of these two techniques, both from a clinical and quantitative morphological standpoint.

## **2.2 Methodology**

### **2.2.1 Patient population**

Between 2004 and 2020, the Pediatric Neurosurgery Unit at IRCCS ISNB in Bologna admitted a total of 43 patients diagnosed with metopic synostosis. We have retrospectively enrolled 10 patients among those, undergone postoperative three-dimensional (3D) stereo-photogrammetry. This retrospective study has received the necessary approvals and endorsements from the local Ethical Committee Board, with reference to code CE 188-2022-OSS-AUSLBO.

Within our unit, we have been using two different techniques for fronto-orbital reshaping. The first technique involves a two-piece frontal craniotomy in conjunction with the application of the fronto-orbital bandeau. This approach is further referred to as "technique A" in the subsequent discussion. Subsequently, we introduced a different approach, namely, forehead remodeling utilizing alternated barrel staving osteotomies and bandeau, hereafter referred to as "technique B."

For the quantitative morphological analysis, the children enrolled, were divided into two groups: group A, comprising those who underwent the double flap technique, and group B, consisting of individuals receiving the barrel staving fronto-orbital remodelling procedure. We only selected children undergone postoperative stereophotogrammetry, distributed as follows: 4 individuals for technique A and 6 individuals for technique B. Furthermore, the results from both groups were compared to a cohort of 10 unaffected children, matched, by age and gender, kindly provided by Rodriguez-Florez et al. (2017) for reference. [71]

## **2.2.2 Surgical techniques**

### **Frontal Bones Transposition and Rotation Technique: "Technique A"**

A straight bicoronal incision is made on the skin, and the scalp flap is carefully elevated, extending up to the supraorbital rim. A periosteal flap is then raised. Dissection is undertaken to locate and safeguard the supraorbital branch of the trigeminal nerve. Subsequently, a frontal craniotomy is performed, commencing from the anterior fontanelle and extending laterally to expose the bone fully, reaching the level of the pterion. The frontal lobes are slightly retracted epidurally to unveil the initial centimeter of the orbital roof, extending from the cranial midline to the pterion. After ensuring the thorough detachment of the periorbita from the superior inner orbital cavity, the fronto-orbital bandeau is removed. The reconstruction of the orbital rim advances through a greenstick fracture in the midline, aligning with the fused suture. Subsequently, the forehead is remodeled by opposing and rotating the frontal bones (see Figure 2). These realigned bones are secured together using absorbable plates, and the newly contoured forehead is affixed to the restructured orbital bony unit similarly. An absorbable X-shaped plate is employed to stabilize all the remodeled bone segments up to the nasion, while two linear plates are fastened on the lateral sides, connecting the new bandeau to the temporal bone (refer to Figure 3). The pericranium is then meticulously sutured to encompass the advanced bony area, and the scalp flap is closed using absorbable sutures in a two-layered fashion. Generally, a subgaleal drain is positioned and remains in place for the initial 48 hours post-surgery.

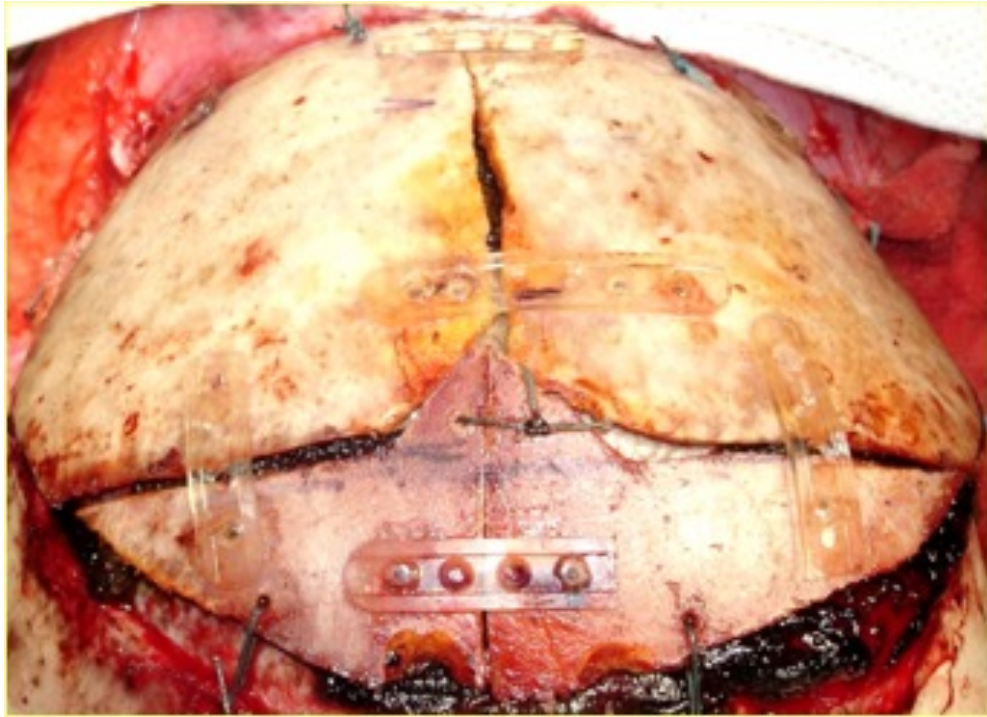


***Figure 2:** the double flap forehead reconstruction, please note that the sides have been swapped in order to achieve a proper roundness of the forehead*

### **Alternated Barrel Staving Technique: "Technique B"**

An undulating bicoronal incision is performed. In comparison to "Technique A," the technique to expose the forehead and the supraorbital rim, is identical. Before initiating the reconstruction phase, bilateral barrel staving osteotomies are conducted in the parieto-temporal bone. These osteotomies are slightly distracted using a bone-bending clamp to facilitate expansion of the central portion of the cranial vault. The orbital rim reconstruction entails fracturing and expanding it at the midpoint, applying a gentle divergent force to the two segments. These segments are then fixed together using absorbable plates. To achieve an upward orientation of the eyebrows, the orbit rims are carefully drilled. Vertical osteotomies, spaced 1.5 cm apart, are made in the frontal bone. The finacuts aid in reshaping the forehead, which is securely fastened into the desired

curvature with the aid of one or two double 20-hole plates on the back side of the bone (see Figure 3).



**Figure 3:** the reconstruction, please note the alternated barrel staving on the forehead flap, and the upper slanting shape of the orbital rim .

The two pieces are subsequently positioned together and attached to the nasion using an X-shaped plate. Two additional fixation points between the forehead and superorbital rim align with the mid-pupillary line, and the rim is ultimately connected to the temporal bone using a lengthy plate on each side. On occasion, these same extended lateral plates are utilized to secure both the forehead and superorbital rim together (refer to Figure 4).

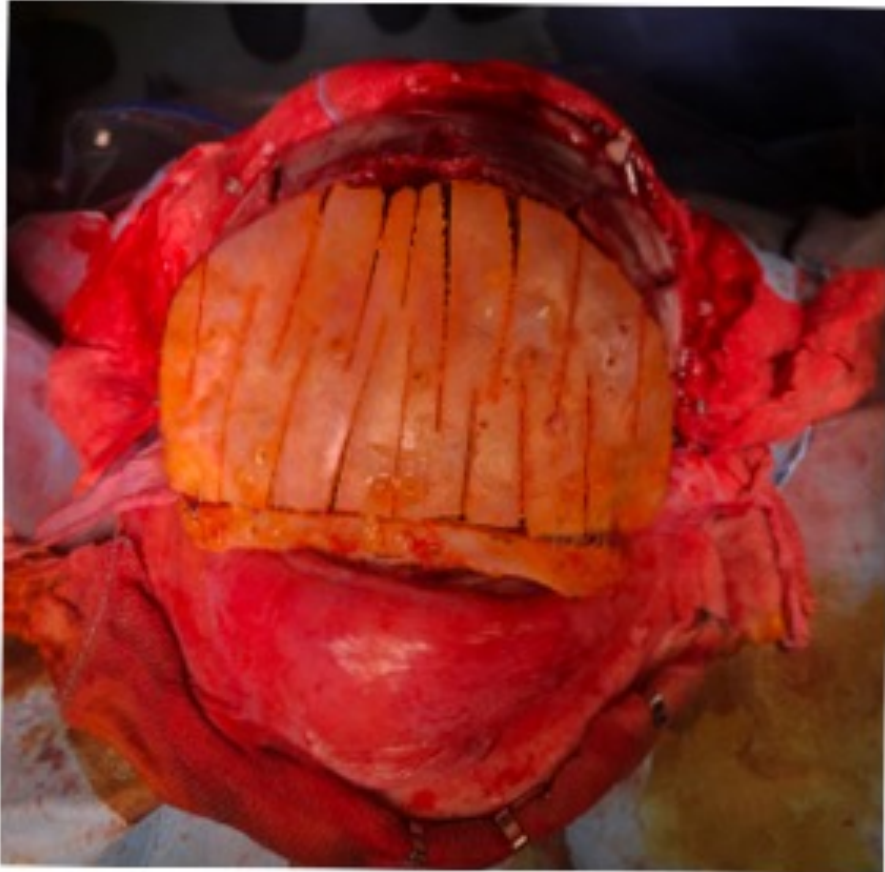


**Figure 4:** *the reconstruction mounted on the patient*

### **Image acquisition**

The surfaces generated from three-dimensional (3D) stereophotogrammetry data, acquired with 3D MD technology, were exported in the stereolithography (STL) format for subsequent processing. All data manipulations were performed by the same operator.

The obtained surfaces were subjected to segmentation to isolate the surgically remodeled portion of the forehead. The segmentation was performed by using MeshMixer Software (Autodesk Inc. based in Toronto, ON, Canada).

The cutting planes employed to crop the interesting region, have been previously described and verified in a study by Rodriguez-Florez et al. (2017) [71].

One of the reference planes passes through the right and left helix and the nasion, representing anatomical features that remain unchanged during surgery. The second plane is then oriented at a  $120^\circ$  angle relative to the first plane, extending posteriorly through the helixes (as illustrated in Figure 5, left panel).

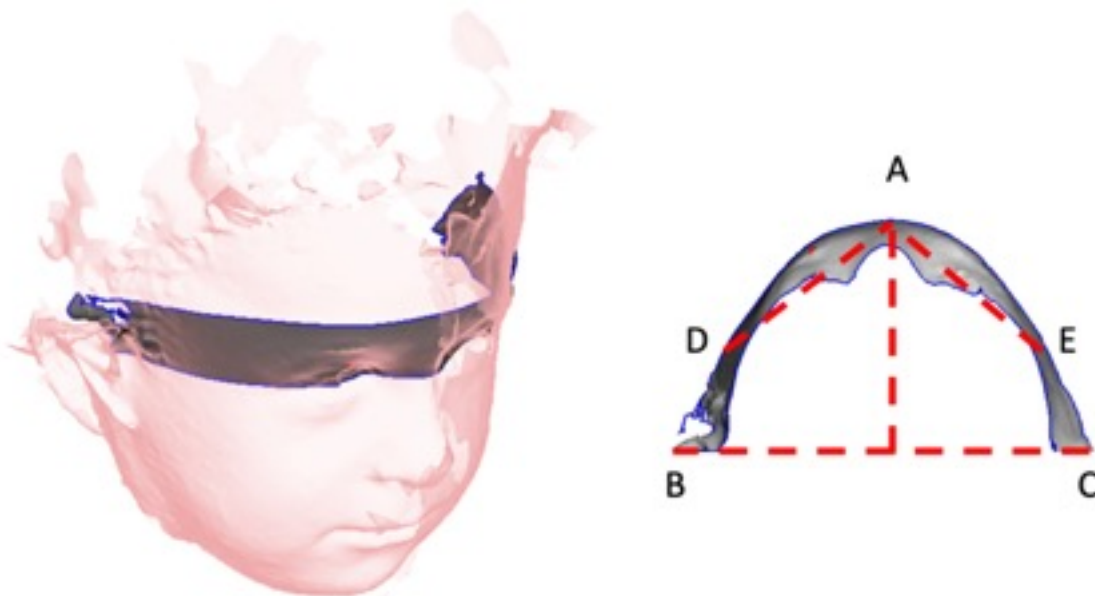


**Figure 5:** the 3D reconstruction of the stereophotogrammetry, please note highlighted the area of interest, on the left, the cephalometric landmarks considered, please refer to the text, on the right

### **Cephalometric measurements**

To evaluate the extent of morphological correction achieved, we conducted measurements of cephalometric landmarks. We considered the interfrontoparietal-interparietal ratio and the frontal angle, both calculated from a plane positioned parallel to the base plane at one-third of the head's height. This

specific plane was selected because it included the most anterior point of the forehead in metopic patients, referred to as point A (situated at the glabella, figure 5 right panel).

The interparietal distance (BC) was defined as the forehead's width, running parallel to the line connecting the left and right crus of the helix. On the other hand, the interfrontoparietal distance (DE) was described as the width of the skull, extending halfway between BC and point A. Consequently, the interfrontoparietal-interparietal ratio was calculated as DE divided by BC. The frontal angle measurement was based on the angles DAE (as depicted in Figure 5, right panel).

Subsequently, we performed a comparative analysis of the cephalometric measurements obtained from the transposition and rotation of frontal bones technique (A) and the alternated barrel staving method (B). Both of these techniques were then compared to measurements obtained from a cohort of children non presenting metopic synostosis, matched by age and gender.

### **2.3 Results**

We recruited a total of 10 patients for this study, with 4 undergoing technique A and 6 undergoing technique B. The median age of these patients at the time of the operation was 7 months. We observed that 6 of them had severe conditions preoperatively, while 4 had conditions classified as mild-severe. None of the patients had mild forms of the condition. During the surgeries, one patient experienced an intraoperative dural tear, which had no

lasting consequences, and two patients developed wound dehiscence, with none requiring a return to the operating room. The average length of hospital stay was 6.7 days (with a standard deviation of 1.9) as shown in Table 1.

Additionally, all patients spent one night in the intensive care unit (ICU).

For all patients, stereophotogrammetry was performed at least one year after the surgery.

Pt	Age At Operation	Length of stay	Complications	Severity	Technique	ratio DE/BC	Frontal angle
1	6 months	5 days		Severe	B	0,791301651	108,8483663
2	7 months	6 days		Mild-severe	B	0,71394722	107,8519571
3	6 months	4 days		Severe	B	0,908542488	98,50662142
4	7 months	7 days	dural tear	Severe	A	0,926319146	93,18315841
5	9 months	9 days		Mild-severe	A	0,775432889	103,8496923
6	6 months	5 days	wound dehiscence	Mild-severe	B	0,76017643	98,82133963
7	7 months	6 days		Severe	B	0,825364093	95,24518232
8	5 months	7 days		Severe	B	0,754373301	102,339888
9	6 months	8 days		Mild-severe	A	0,871647057	105,0230495
10	26 months	10 days	wound dehiscence	Severe	A	0,825330634	85,55212391

**Table 1:** demographic details of the patients of the study group, alongside with the measurements details

### 2.3.1 Cephalometric measurements

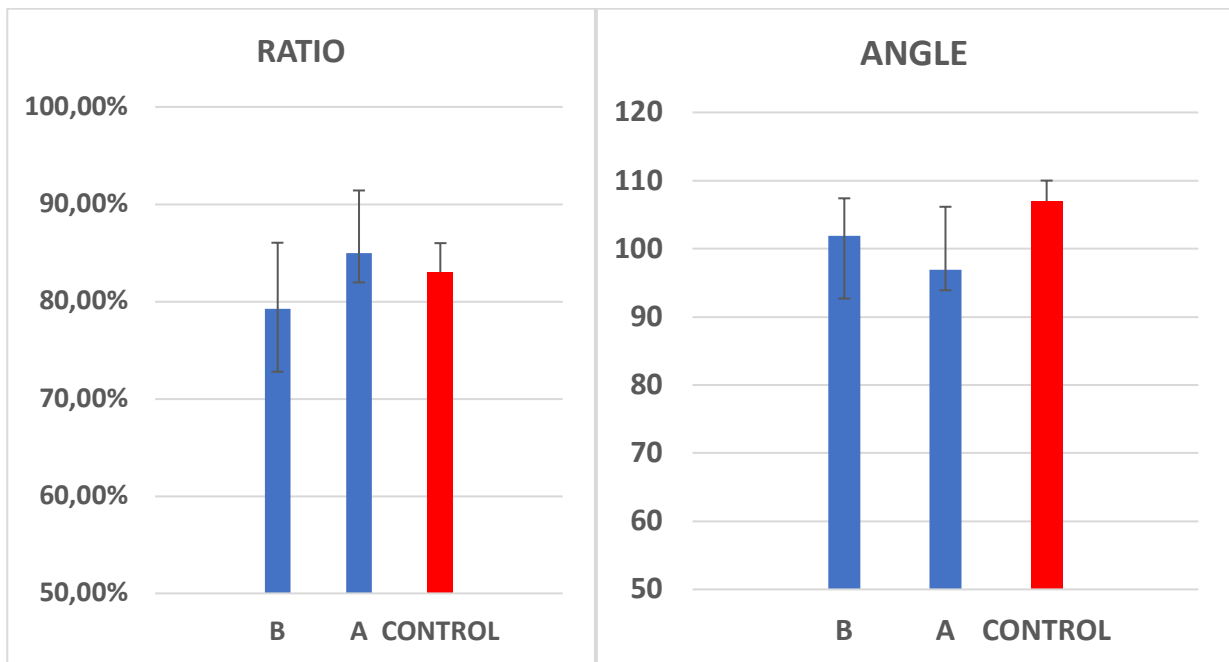
The mean and standard deviations of the cephalometric measurements, including the interfrontoparietal-interparietal ratio and frontal angle, are presented in Table 2.

**Table 2:** in the first column patients (PT) are indicated by numbers, second column the technique (TEC) is indicated, followed by the measurements obtained for ratio DE/BC and the frontal angle.

At the bottom of the table, please find means and standard deviation for each group comprehended the control group of unaffected patients.

Regarding the interfrontoparietal-interparietal ratio (DE/BC), no significant differences were observed between the A group and the control group. The mean interfrontoparietal-interparietal ratio was 79.2% in the B group and 84.97% in the A group, whereas the control group had a mean of 83%. The corresponding p-values for comparing the control group to the A technique ( $p = 0.4747$ ) and the B technique ( $p = 0.095$ ) were not statistically significant.

For the frontal angle measurements, the B group exhibited a mean of  $101.94^\circ$ , while the A group reported a mean of  $96.9^\circ$ . In contrast, the control group had a mean frontal angle of  $107^\circ$  (refer to Graph 1). The p-values for the frontal angle comparison were 0.0257 for the A technique and 0.0822 for the B technique.



**Graph 1:** on the left please note the histogram of the ratio DE/BC. Both techniques correct the ratio which clinically indicated the frontal width with the B technique slightly undercorrecting this area, whereas the angle is best corrected by the B technique rather than the A.

### 2.3.2 Clinical outcomes

Out of the 43 patients who underwent surgical treatment, only one case received minimally invasive treatment, while the remaining cases underwent open remodeling of the forehead and supraorbital rim. Among these patients, two individuals required secondary surgeries, performed 7 and 9 years after the primary operation, respectively. In one case, the Authors reported a recurrence of the trigonocephalic shape, while the other child developed signs of increased intracranial pressure.

During the secondary surgery, an intraoperative dural tear occurred in the latter case, resulting in the accumulation of cerebrospinal fluid (CSF) that required the placement of a temporary shunt. Regrettably, this same child

experienced complete blindness in the right eye, despite the absence of radiological evidence indicating thrombosis in ophthalmic and retinal veins.

Additionally, six cases presented with noticeable speech delays during their pre-school years.

## **2.4 Discussion**

Minimally invasive techniques, which have been successfully applied in other forms of single-suture craniosynostosis, and in some cases for trigonocephaly, have not gained widespread acceptance for the correction of metopic synostosis. This is primarily due to the complex morphological changes involved, which extend beyond the characteristic trigonocephalic shape of the frontal bone. [72-75]

Various open techniques have been described for correction, including forehead reshaping with or without addressing the upper part of the orbits [72-75], as well as correction of hypotelorism through bone graft insertion [76]. Unfortunately, a degree of relapse in terms of flattening and the wedge-shaped forehead is a common complication after surgery. Consequently, many surgeons opt for hypercorrection. This tendency toward relapse has been associated with the early age at which correction is typically performed, usually advised between 6 and 12 months of life [77-78]. It's worth noting that younger children are at a higher risk of premature cranial closure and a recurrence of the trigonocephalic shape.

At our center, we perform surgery on all primary trigonocephaly patients after they reach 6 months of age. This timing allows for sufficient bone stiffness

to ensure implant stability while preserving the child's natural bone regenerative capacity.

With technique A, the metopic ridge disappears over the long term but is eventually replaced by a noticeable forehead ridge. On the other hand, the alternated barrel staving technique (technique B) has yielded better results in terms of maintaining frontal roundness and a lasting correction of the metopic ridge over time.

Our cephalometric analysis of 3D forehead shapes indicates that technique B (alternated barrel staving) has greater correction power regarding the angle of metopic synostosis, whereas technique A (transposition and rotation of frontal bone flaps) achieves a broader correction of frontal stenosis, resulting in a greater interfrontoparietal-interparietal ratio (DE/BC ratio). However, it's important to note that both reconstruction methods did not show statistically significant differences when compared to the control group.

Based on our experience, we prefer to focus on addressing the frontal angle and aim for a slightly under-corrected interfrontoparietal width to prevent forehead flatness. In general, our cephalometric measurements on metopic patients after fronto-orbital remodeling indicate that surgery effectively improves trigonocephaly, as evidenced by the increased interfrontoparietal-interparietal ratio and widened frontal angle. Similar findings have been reported in measurements taken from CT scans and 3D photos of metopic patients who underwent various fronto-orbital remodeling procedures.

## **2.5 Conclusion**

In our experience, we observed that the barrel-staving technique achieved a more significant correction of the frontal angle compared to the transposition of two frontal bone flaps with resorbable median fixation. This was despite achieving a less substantial correction in interfrontoparietal width. When deciding on the most suitable technique, we believe that a degree of undercorrection in the interfrontoparietal diameter has a milder aesthetic impact compared to undercorrection of the metopic angle, which is a primary goal of this surgical procedure.

However, it's essential to emphasize that definitive conclusions should not be generalized, and the choice of the surgical approach for treating trigonocephaly should always consider the individual's age and the specific type and severity of the deformity.

**Chapter 3 OBJECTIVE 2**

**PRECLINICAL APPLICATION OF**

**HOLOLENS2**

### **3.1 Rationale of the Survey**

Having chosen the fronto-orbital remodeling for trigonocephaly as the technique that we wanted to test preclinically with AR, and due to the fact that HoloLens2 are not considered a medical device, we had to test them first in a controlled experimental environment.

In this study, the Authors assess the accuracy of AR guidance employing the commercially available HoloLens 2 Head-Mounted Display (HMD) [80] to perform fronto-orbital remodeling (FOR) to correct metopic synostosis, in an experimental setting, with a 3D printed phantom.

## **3.2 Material and Method**

### **3.2.1. Methodology**

The study was structured to first implement the AR-based protocol utilizing the HoloLens 2 smart glasses. Subsequently, the authors conducted a test session to assess the effectiveness of AR-guided osteotomies during fronto-orbital remodeling (FOR) procedures on a 3D printed phantom.

### **3.2.2. Development Phase**

#### **Virtual Content Preparation**

We chose the preoperative CT scan data of a previously admitted and operated patient presenting metopic synostosis, adhering to the study protocol CE 499-2022-OSS-AUSLBO. The DICOM data were acquired and segmented to create a three-dimensional (3D) virtual model of the patient's skull. Various anatomical parts within the patient's head were segmented utilizing Mimics (Materialise in Leuven, Belgium). These parts included bones, brain, eye globes, and skin. Subsequently, 3D meshes were generated based on the segmented masks and were saved in the Standard Tessellation Language (STL) format (refer to figure 6 for illustration).

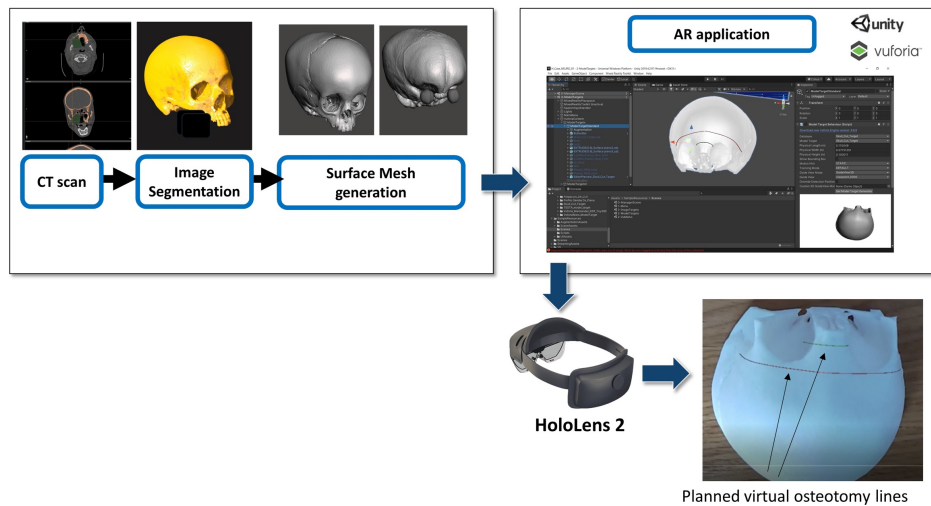


**Figure 6:** Segmentation of the CT scan to obtain the virtual 3D skull model, then 3D printed to obtain a patient-specific phantom. On the virtual skull model the osteotomies are designed and then navigated by means of HMD.

### 3D Printing of Skull Phantom and CAD/CAM Templates for Accuracy

#### Assessment

To evaluate the accuracy of AR guidance, a specific section of the reconstructed skull was chosen for printing. In line with clinical data, we opted to visualize the skull from a top-down perspective, mimicking the view in an actual surgical setting. The model was defined by cuts behind the coronal sutures and bilaterally at the level of the fronto-zygomatic sutures, in order to maintain only the part of the skull which is exposed during the actual procedure.

Using the cut STL file, a phantom model was created using photosensitive resin through stereolithography (SLA) 3D printing technology (Form 3, Formlabs, Somerville, MA, USA). In order to assess the accuracy of AR guidance, CAD/CAM templates were designed using MeshMixer software (Autodesk Inc., CA, US), accordingly to the planned osteotomies. These templates were meant

to be placed on the surface of the phantom model, serving to assess the position of the planned FOR osteotomies.

For the AR-guided task, we specifically chose the nasal osteotomy of the orbital rim within the context of fronto-orbital remodeling, along with the upper limit of the rim (refer to figure7, left). The templates of the cutting guides were also 3D printed (Form 3, Formlabs), incorporating grooves of varying widths (3 mm, 2 mm, 1 mm). This allowed us to evaluate accuracy across three different levels:  $\pm 1.5$  mm,  $\pm 1.0$  mm, and  $\pm 0.5$  mm (as in figure 7, right).

To measure accuracy, a millimeter adhesive tape was associated with each template, facilitating the assessment of the cumulative length of the traced osteotomy within the grooves. We deemed the AR-guided task successful (achieving a 100% success rate) when the traced osteotomy profile consistently aligned with and remained within the groove of the cutting guides along their entire length. For instance, in the case of the nasal osteotomy, the target length was 27 mm, while for the frontal osteotomy, it was 75 mm.

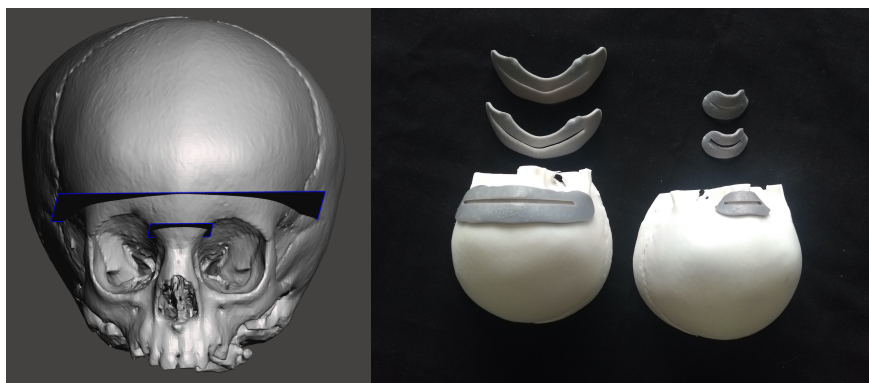


**Figure 7:** On the left, the planned osteotomies for the fronto-orbital bandeau of the FOR, on the right the 3D printed cutting guides with calibrated grooves for both osteotomies.

## **Development of the Augmented Reality (AR) Application**

The virtual model of the skull, incorporating all its components such as bones, skin, eye globes, and brain, was introduced into the Unity 3D software. This software was further augmented with a specialized software development kit designed for creating augmented reality applications, Vuforia Engine package (PTC, Inc., Boston, MA, USA).

The Vuforia Engine software allowed the AR interface, by aligning the holograms the model of the skull. This alignment was realized using the "Model Target" function, which enabled the system to recognize the shape of an actual object that needed to be tracked. To accomplish this, the object had to be observed from a specific view. In our case, we opted to replicate the surgeon's viewpoint during the fronto-orbital remodeling procedure within the operating theater. The AR application projected a profile known as the "guide view" of the Model Target. The user simply had to adjust the lenses until the projected drawing aligned with the actual object.

In this study, the 3D model of the patient's skull served as the Model Target for the registration of the virtual-to-real scene. The AR application generated multiple holograms overlaying the printed portion of the skull, each corresponding to a specific structure, such as the bony skull, skin, brain, eye globes, and the planned FOR osteotomy trajectories. These holograms served as visual guides during the surgical task.

The resulting AR application was developed as a Universal Windows Platform (UWP) app, intended for deployment on Microsoft HoloLens 2 smart glasses. To enhance user interaction, a box with checkboxes were incorporated into the

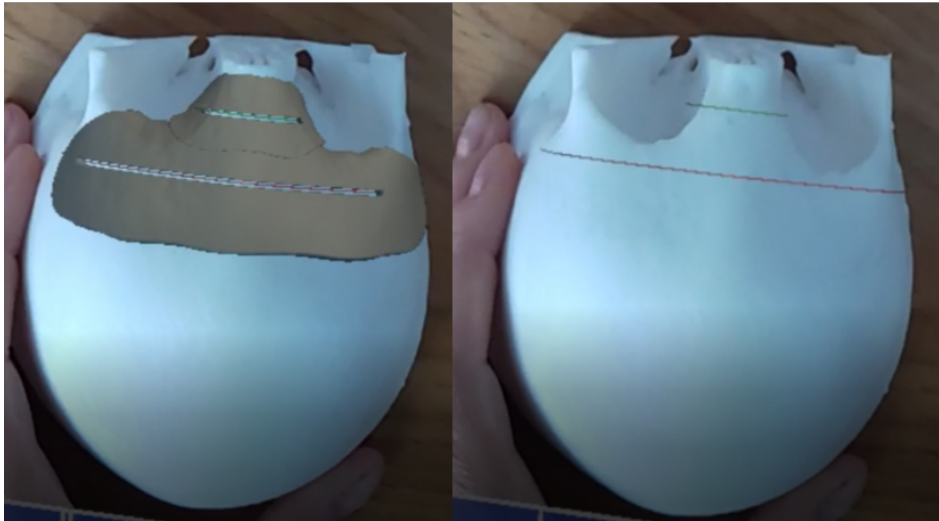
user interface, allowing the user to toggle the rendering of individual virtual anatomical structures and the planned virtual osteotomy trajectories on and off. Furthermore, voice commands were implemented to enable a hands-free AR guidance system, granting additional convenience and flexibility to the user.

### **3.2.3. Experimental Phase**

To evaluate the performance of the AR application on HoloLens 2, the authors conducted trials involving the selected FOR osteotomies, specifically the nasal osteotomy and the frontal osteotomy, measuring 27 mm and 75 mm in length, respectively. These osteotomies were carried out under the guidance of the AR application.

A total of six participants were recruited, three surgeons and three engineers (an equal mix of males and females) ranging in age from 25 to 50 years. Each participant repeated the procedure six times using the same 3D printed phantom, with a one-week interval between each trial. Prior to commencing the task, participants were given detailed instructions on the objectives of the experiment

1. Virtual templates and planned osteotomies superimposed on the skull phantom



2. Execution of AR-guided task

3. Check for accuracy using templates



**Figure 8 (clockwise):** user's visualization with cutting guide hologram (left) and osteotomies (right)

Participants initiated the AR-guided task after calibrating the Head-Mounted Display (HMD) for optimal hologram perception. The users had to enable tracking through the Model Target tracking function and then proceeded with the AR-guided osteotomy task. Utilizing a pencil, participants traced the osteotomy trajectories onto the skull phantom, following the holograms guidance. Vocal commands were available to participants, allowing them to reveal or conceal virtual structures during the task (figure 8).

Subsequently, another operator, using the 3D printed templates designed for accuracy assessment, evaluated the extent to which the lines traced under AR guidance aligned with the grooves in the individual templates. Each template featured a calibrated tape along the groove, simplifying the measurement process.

#### **3.2.4. Statistical Analysis**

Data from all measurements were documented. Percentages were calculated, and the measurements underwent statistical analysis, including the Kruskal-Wallis test and the Mann-Whitney test.

For conducting the statistical analysis, SPSS software (IBM, Armonk, New York, USA) was employed, and a significance level of  $<0.05$  was considered.

### **3.3 Results**

The outcomes are reported in Table 3. When using HoloLens 2, 97% of users successfully traced the osteotomy trajectory with an accuracy level of  $\pm 1.5$  mm, as verified with the "3mm" template, for the nasal cut. However, this percentage decreases to 80% when considering the frontal cut. For accuracy levels of  $\pm 1$  mm and  $\pm 0.5$  mm, lower success rates were observed. Specifically, for the nasal cut, success rates were 80% and 61%, respectively. In the case of the frontal cut, users achieved the task with an accuracy level of  $\pm 1$  mm in 52% of instances, while only 33% drew the line in the groove with an accuracy level of  $\pm 0.5$  mm.

NOSE				FRONTAL			
PT 1	CG (3 mm)	CG 2 (mm)	CG 1 (mm)	PT 1	CG (3 mm)	CG	
2 (mm)	CG 1 (mm)						
		1	27 mm 27 mm 24 mm	1	75 mm 70 mm	40 mm	
		2	27 mm 27 mm 27 mm	2	75 mm 75 mm	55 mm	
		3	27 mm 25 mm 23 mm	3	75 mm 75 mm	60 mm	
		4	27 mm 24 mm 22 mm	4	75 mm 72 mm	65 mm	
		5	27 mm 27 mm 27 mm	5	70 mm 70 mm	60 mm	
		6	27 mm 26 mm 25 mm	6	75 mm 75 mm	75 mm	
PT 2				PT 2			
		1	27 mm 26 mm 23 mm	1	75 mm 55 mm	35 mm	
		2	27 mm 27 mm 26 mm	2	75 mm 75 mm	75 mm	
		3	27 mm 27 mm 27 mm	3	75 mm 73 mm	55 mm	
		4	27 mm 27 mm 27 mm	4	75 mm 75 mm	74 mm	
		5	27 mm 27 mm 25 mm	5	75 mm 75 mm	75 mm	
		6	27 mm 27 mm 27 mm	6	75 mm 75 mm	35 mm	PT 3
				PT 3			
		1	27 mm 25 mm 20 mm	1	75 mm 75 mm	70 mm	
		2	27 mm 27 mm 27 mm	2	75 mm 71 mm	75 mm	
		3	27 mm 27 mm 27 mm	3	75 mm 75 mm	70 mm	
		4	27 mm 27 mm 27 mm	4	75 mm 75 mm	75 mm	
		5	27 mm 27 mm 27 mm	5	75 mm 70 mm	60 mm	
		6	27 mm 27 mm 27 mm	6	75 mm 70 mm	35 mm	
PT 4				PT 4			
		1	27 mm 27 mm 27 mm	1	75 mm 75 mm	65 mm	

	2	27 mm	15 mm	10 mm	2	75 mm	75 mm	75 mm
	3	27 mm	27 mm	26 mm	3	75 mm	75 mm	75 mm
	4	27 mm	27 mm	22 mm	4	75 mm	70 mm	55mm
	5	27 mm	27 mm	27 mm	5	73 mm	71 mm	65 mm
	6	27 mm	27 mm	27 mm	6	70 mm	60 mm	60 mm
PT 5					PT 5			
	1	27 mm	27 mm	27 mm	1	70 mm	50 mm	35 mm
	2	27 mm	27 mm	27 mm	2	70 mm	65 mm	55 mm
	3	20 mm	12 mm	11mm	3	65 mm	45 mm	35 mm
	4	27 mm	25 mm	25 mm	4	75 mm	59 mm	54 mm
	5	27 mm	27 mm	27 mm	5	75 mm	75 mm	45 mm
	6	27 mm	27 mm	27 mm	6	75 mm	57 mm	45 mm
PT 6					PT 6			
	1	27 mm	27 mm	27 mm	1	75 mm	75 mm	75 mm
	2	27 mm	27 mm	27 mm	2	65 mm	60 mm	55 mm
	3	27 mm	27 mm	27 mm	3	75 mm	75 mm	75 mm
	4	27 mm	27 mm	27 mm	4	75 mm	75 mm	75 mm
	5	27 mm	27 mm	27 mm	5	75 mm	75 mm	75 mm
	6	27 mm	27 mm	27 mm	6	75 mm	75 mm	75 mm

**Table 3:** Measurements taken from each recruited user: on the left column the measurements for the nasal cut; on the right column measurement for the frontal cut. CG: cutting guide

The Kruskal-Wallis test revealed that all users effectively completed the nasal cut task, with no significant differences among them. However, the frontal cut

exhibited more variations between operators (see Table 4). Only one outlier was detected in the measurements through a Mann-Whitney test (see Table 5).

Test Statistics <sup>a,b</sup>						
	fro 3 mm	fro 2mm	fro 1mm	nos 3mm	nos 2mm	nos 1mm
Kruskal-Wallis H	6.992	9.579	13.083	5.000	4.883	6.521
df	5	5	5	5	5	5
Asymp. Sig.	.221	.088	.023	.416	.430	.259

a. Kruskal Wallis Test  
 b. Grouping Variable: operator

**Table 4:** Kruskal Wallis Test, demonstrating no significant difference between operators

Test Statistics <sup>a</sup>															
Z	op2 - op1	op3 - op1	op4 - op1	op5 - op1	op6 - op1	op3 - op2	op4 - op2	op5 - op2	op6 - op2	op4 - op3	op5 - op3	op6 - op3	op5 - op4	op6 - op4	op6 - op5
Asymp. Sig. (2-tailed)	.752	.498	.293	.043	.066	.357	.225	.074	.174	.680	.046	.343	.027	.414	.041

a. Wilcoxon Signed Ranks Test  
 b. Based on negative ranks.  
 c. Based on positive ranks.

**Table 5:** Mann Whitney test, only one outlier between the operators is evident

The users found the AR guidance system highly usable, but a majority of them noted a perceived reduction in image quality when maneuvering the pencil in front of the visor.

### 3.4. Discussion

AR technology holds great promise in the medical field, with a growing number of studies exploring its applications, particularly in surgery [4,5,14, 22-29, 81-83]. AR enhances surgical navigation by allowing the surgeon to maintain focus on the patient while overlaid holograms provide essential information directly on the patient [25].

AR HMDs are categorized as optical see-through devices or video see-through devices [23-25,27,28,79]. This study specifically employed HoloLens 2, an optical see-through HMD.

Craniofacial surgeries, particularly those addressing forehead anomalies need accurate execution of osteotomies, for achieving optimal results. HoloLens has shown promise in this regard [13]. However, the technology does have limitations, such as depth perception and registration errors [79,82,83]. Our previous work attempted to address these limitations, reporting static errors ranging from 1 to 10 mm, resulting in a misalignment between the virtual and real images [84].

This study evaluated the accuracy of HoloLens 2 in craniofacial surgery, specifically fronto-orbital remodeling, focusing on two critical osteotomies: the nasal and frontal cuts. Six operators participated, each performing the task six times for both osteotomies, with a one-week interval between trials to minimize any learning curve effect. The users traced the osteotomies with a pen guided by HoloLens 2 projections, which displayed the phantom and lines representing the planned osteotomies. Alignment errors and reduced sharpness were observed when moving the pen in the field of view. Nevertheless, all users successfully completed the task, and the traced osteotomies were checked against cutting guides with different groove widths to assess accuracy.

Our accuracy findings are consistent with what found elsewhere in Literature [13,24,25,85, 86]. Scherl et al. reported accuracy of less than 1.3 mm in their in vivo study [24, 25], while Tang et al. described mean deviation of  $1.68 \pm 0.92$

mm between preoperative virtual osteotomy planes and actual postoperative planes, with the largest deviation being 3.46 mm [87]. Han et al. reported promising results in craniosynostosis patients undergoing calvarial remodeling [88].

In our study we perceived an overall good users' experience, but we report some limitations. These limitations encompassed registration errors and a small augmentable field of view. While sub-millimetric precision was essential for our task, other "surgery-specific" devices may be required for more complex procedures, as described in the existing literature [27, 84].

Despite its limitations, our study showed encouraging results based on 36 phantom procedures, with only one outlier. However, several factors influenced our findings, including favorable lighting conditions compared to real surgical settings, Model Target registration errors, and operator-dependent variables. Our next step involves enhancing the navigation system by incorporating more detailed 3D objects for simultaneous visualization with instrument-guided trajectories (i.e., osteotomies). The preparation time, involving 3D model reconstruction from DICOM data segmentation and AR guidance software setup, was relatively efficient, taking approximately one to two hours, excluding the printing time [84]. Subsequent in vivo studies will be crucial for confirming these preliminary findings.

### **3.5. Conclusions**

This study is conducted in a controlled experimental setting (in vitro). The promising outcomes regarding accuracy within a range of  $\pm 1.5$  mm suggest the potential suitability of this technology for application in craniofacial surgery,

considering that an error of 2 mm in this surgical specialty is acceptable. However, further research, including in vivo assessments, is necessary to address and refine the technical challenges.

**Chapter 4 OBJECTIVE 3:**  
**APPLICATION OF HOLOLENS2**  
**IN A CLINICAL SETTING**

#### **4. Rationale of the survey**

Our research group has previously explored the potential of AR HMDs, specifically using Microsoft's HoloLens 2, in craniofacial surgery through preclinical applications on phantoms [13]. In this study, which constitutes the third part of this doctoral project, we present a case series involving the first craniofacial patients treated with the assistance of AR HMD technology. We compare the accuracy of drawing osteotomy trajectories under the guidance of AR HMDs and traditional surgical navigation systems. These findings represent our experience in in vivo clinical practice.

#### **4.2 Materials and Methods**

Our study was designed to implement the AR-based protocol on HoloLens 2 smart glasses within the real operating room environment. Subsequently, these AR HMDs were utilized during surgical procedures to guide the drawing of osteotomy lines. These drawings were then compared to lines traced with the standard neurosurgical navigator, known as Stealth 7 by Medtronic. This comparison was facilitated using 3D printed cutting guides. The subsequent sections detail both the development phase and the experimental phase of our study.

## **4.2.1. Development Phase**

### **4.2.1.1. Virtual Content Preparation**

We initiated our study by utilizing a preoperative CT scan from patients undergoing corrective surgery for single suture craniosynostosis. Starting from the DICOM data obtained by each CT scan, and employing Mimics software (Materialise, Leuven, Belgium), we created three-dimensional (3D) virtual models of the patients' skull. We also uploaded on the virtual model the osteotomy lines of the virtual surgical planning, in STL format.

### **4.2.1.2. 3D Printing of CAD/CAM Cutting-Guides for Testing Accuracy**

To evaluate the precision of the AR guidance system, we designed CAD/CAM templates using Autodesk Inc.'s MeshMixer software (CA, US). These templates were strategically positioned on the patient's body, aligning with planned osteotomy locations (visualized in the figure). These templates were then manufactured using 3D printing technology (Form 3, Formlabs) and featured grooves of varying widths (3 mm and 2 mm). These different groove sizes allowed us to assess three distinct levels of achievable accuracy:  $\pm 1.5$  mm and  $\pm 1.0$  mm, as depicted in Figure 9.



**Figure 9:** *intraoperative aspect of one of the CAD-CAM cutting guides*

We defined a task as successfully completed (with a 100% success rate) when the traced osteotomy profile remained entirely within the groove of the cutting guides along its entire length.

#### **4.2.1.3. The AR Application**

The virtual model of the skull, complete with its various components (including bone, skin, osteotomy lines and cutting guides), was imported into Unity 3D (Unity Technologies San Francisco, CA, USA). To enhance its capabilities for creating augmented reality applications, we integrated a specific software development kit known as the Vuforia Engine (PTC, Inc. Boston, MA, USA).

Through the Vuforia Engine software, we achieved alignment between the virtual osteotomy and the physical skull using the "Image Target" function. This

function enables the system to recognize the QR code on the object (in this case patient) that needs to be tracked. To accomplish this, the object must be viewed from a specific angle, replicating the surgeon's perspective during a craniofacial procedure while wearing the AR glasses.

In this research, the AR environments were created using Unity3D version 2019.4.21f1 (Unity Technologies located in San Francisco, CA, USA). To bring in all the virtual models of interest, we integrated the Vuforia Engine Software Development Kit (PTC Inc. in Boston, MA, USA).

The Vuforia Engine leverages the principles of feature tracking and matching in computer vision to identify and track objects and images in the real world. It then renders corresponding virtual objects based on their orientation relative to these real-world objects.

The AR application was developed as a Universal Windows Platform (UWP) app and deployed on Microsoft HoloLens 2 smart glasses. To provide an interactive user experience, we incorporated toggles in the user interface, in the form of checkboxes, allowing users to enable or disable the rendering of individual virtual anatomical structures and planned virtual osteotomy trajectories. Additionally, we implemented voice commands to facilitate a hands-free AR guidance system, enabling users to show or hide the virtual structures using voice control. On the side, we also implemented a system for remote control.

#### **4.2.1.4. Image Target Tracking**

In contrast to our previous work, we utilized Image Target Tracking for these cases. Image Target Tracking, a prevalent tracking technique employed in the Vuforia Engine, relies on recognizing and tracking a predefined image, often taking the form of a QR-code pattern. The Vuforia Engine identifies and tracks this image by comparing naturally extracted features from the camera image with the preselected Image Target, which has been previously chosen for tracking performance and stored within a cloud database. Users can access and download the chosen Image Target from the database as a package that can be integrated into their Unity application.

#### **4.2.1.5. Experimental Phase**

The authors assessed the AR application for HoloLens 2 by drawing osteotomies for craniofacial surgery and comparing them with those drawn under the guidance of the standard navigator.

The study received approval from the local ethical committee (CE AVEC 499-2022-OSS-AUSLBO).

We enrolled 10 consecutive pediatric patients undergoing corrective surgeries for craniosynostosis. These patients were admitted from September 2022 to September 2023 at the Regional Center for Pediatric Neurosurgery IRCCS Istituto delle Scienze Neurologiche di Bologna.

One of the surgeons initially traced the planned osteotomy under the guidance of the standard navigator, drawing a dotted line on the patient's skull. Subsequently, they drew the same osteotomy line after calibrating the HMD for optimal hologram perception, using QR code tracking (figure 10). The surgeon then drew the osteotomy line under AR guidance as a continuous line. After each drawing, another operator assessed the accuracy of both lines using the calibrated CAD-CAM templates. An additional operator captured photographs of the cutting guides on the patients. Three independent operators then measured the percentage of the drawn osteotomy line that fell within the grooves of the cutting guides.

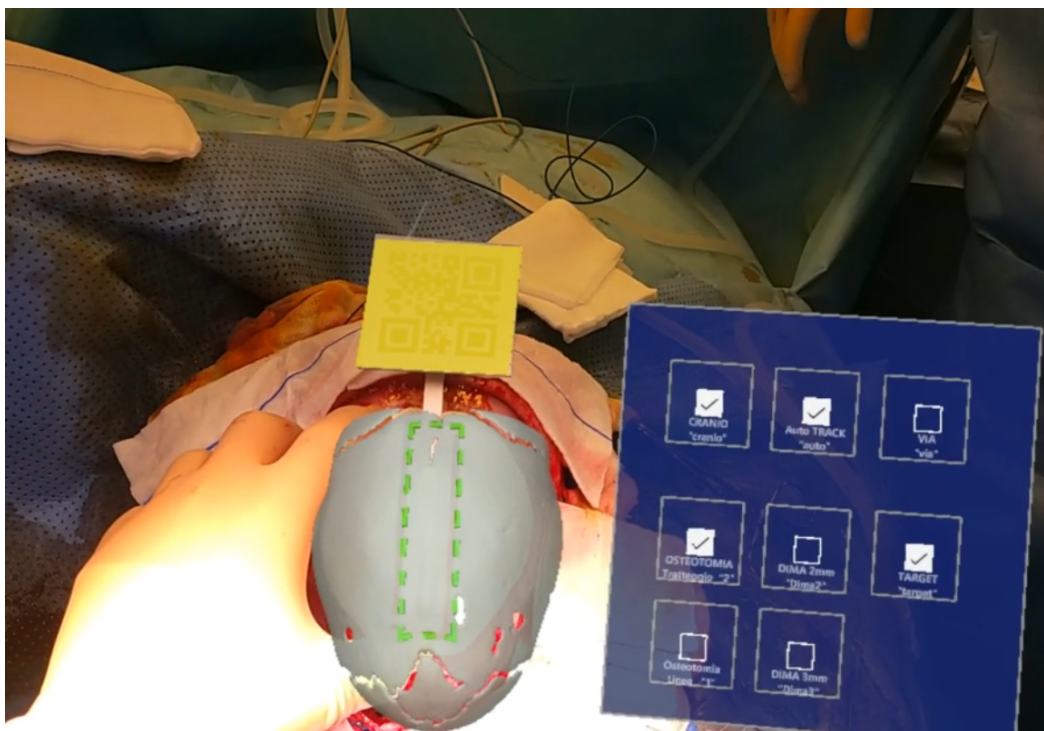


**Figure 10:** intraoperative view of the QR code tracking

Of all of the patients included, we selected simple tasks to test AR vs Navigator. We selected some osteotomies both for the FOR and the sagittal suturectomy (please see fig. 11)

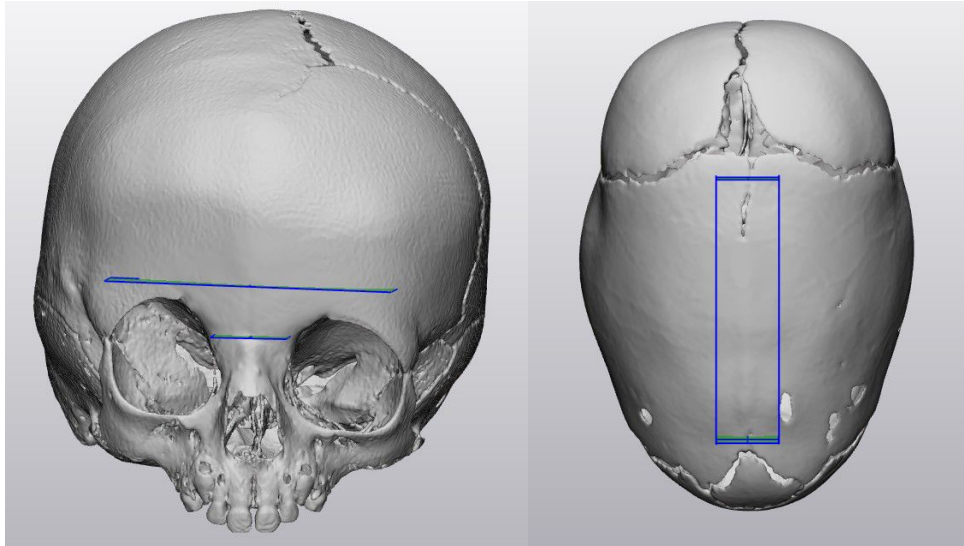


**Figure 11:** on the left, the surgical planning and the osteotomies selected for the FOR, on the right side the osteotomies selected for the sagittal suturectomy

#### **4.2.2. Statistical Analysis**

Data from all measurements were documented. Percentages were calculated, and the measurements underwent statistical analysis, including Student T test for independent data.

The Authors used the SPSS Software (IBM, Armonk, New York, USA) for statistical analysis, and considered a significance level of  $<0.05$ .

### 4.3. Results

Patients age ranged from 4 to 44 months, median 8 months. We enrolled 5 females and 5 males. 4 patients underwent FOR, 4 sagittal suturectomy (SAG), 1 a posterior vault expansion (PVE) distraction and 1 had a total calvarial remodeling (TCR) (demographic description of the patients is in table 6). All patients had preoperative CT scans, and they all experienced a normal postoperative course. 4 of them had auto-resolving minor complications (such as dural tear and wound dehiscence), all Type 1 by Clavien Dindo. The hospital in-stay ranged from 4 to 15 days, median 5 days. All patients were admitted at least for one night in ICU, as per anesthesia protocol.

Pt	Gender	Age at surgery	Complications	Procedure	Inhospital stay
1	F	7		FOR	5
2	M	44	dural tear wound	PVE	15
3	F	4	dehiscence	SAG	7
4	M	8	dural tear	SAG	4
5	M	4		SAG	5
6	M	33		TCR	6
7	F	7	dural tear	FOR	6
8	M	10		SAG	4
9	F	9		FOR	5
10	F	12		FOR	5

**Table 6:** enrolled patients, the age is in months.

Three independent researchers measured which was the extent of the osteotomy line falling into the groove for each navigation method. (figure 12). For the measurements we only included 8 out of 10 patients, because the first two patients did not have the comparison with the Navigation system.

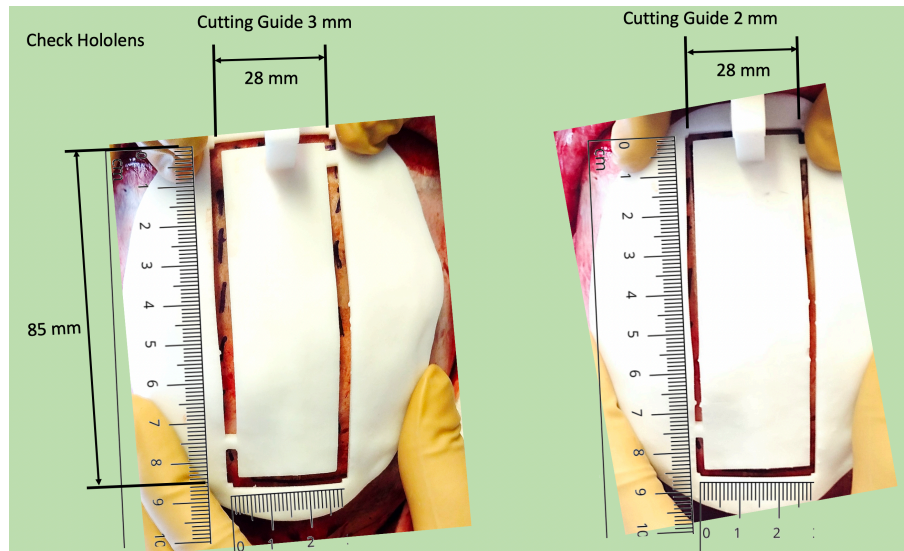


**Figure 12:** this is the graphical representation of how the measurements have been taken

We registered a total of 67 measurements for each domain: Navigator (NAV) for accuracy level of 3 mm, Navigator (NAV) for accuracy level of 2 mm, Augmented Reality (AR) for accuracy level of 1.5 mm and Augmented Reality (AR) for accuracy level of 1 mm.

The results from the descriptive statistical analysis are summarized in Table 7. With HoloLens 2, the surgeons were able to trace an average of 45% measured on all determinations (standard deviation SD 0.4) of the entire length of the osteotomy line within an accuracy level of 1.5 mm. This percentage decreased to 34% (SD 0.3) when considering an accuracy level of 1 mm.

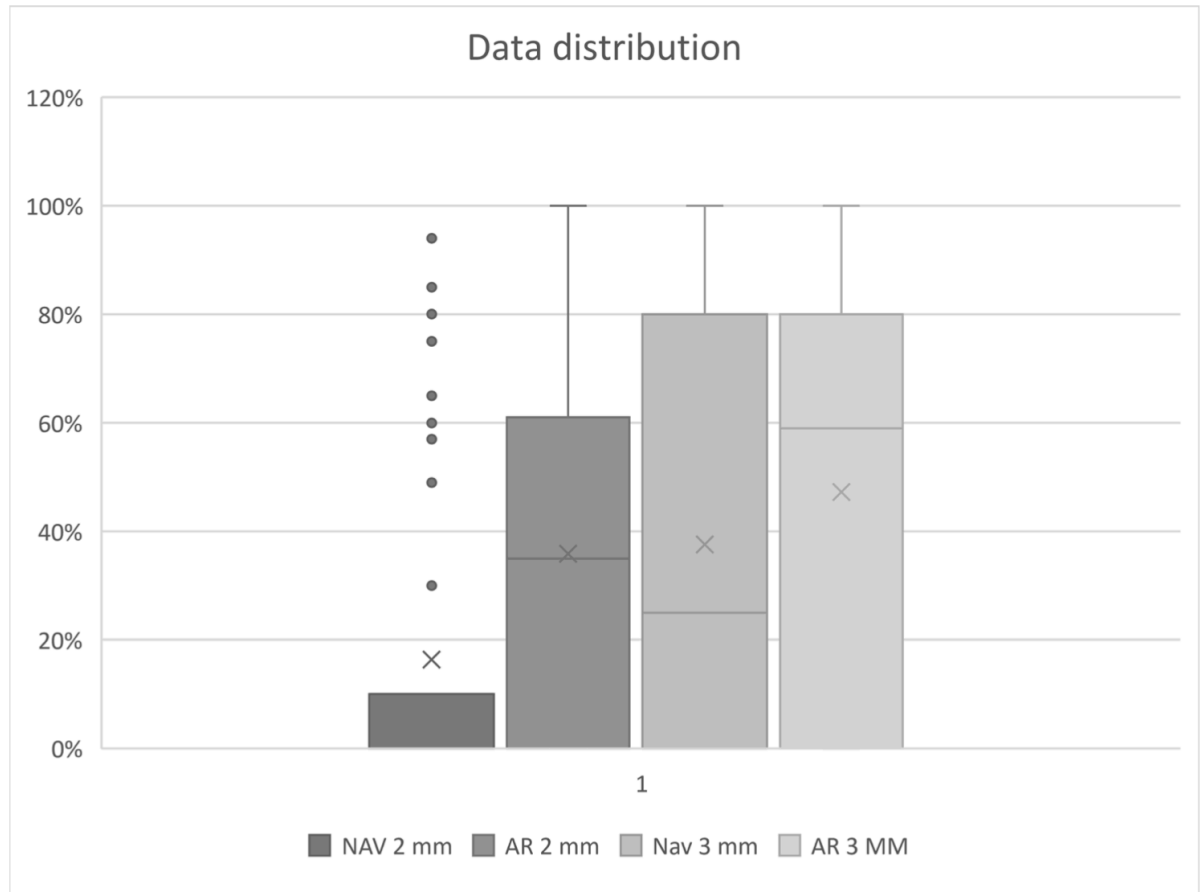
	<b>1.5 mm</b>		<b>1 mm</b>	
	<b>Mean</b>	<i>SD</i>	<b>Mean</b>	<i>SD</i>
<b>NAV</b>	<b>36%</b>	<i>0.4</i>	<b>16%</b>	<i>0.3</i>
<b>AR</b>	<b>45%</b>	<i>0.4</i>	<b>34%</b>	<i>0.3</i>

**Table 7:** descriptive analysis of the direct comparison between AR and Navigator (NAV)

In comparison, when using the benchmark for comparison—the neurosurgical navigator—the operator was able to trace on average the 36% of the line (SD 0.4) for the 3 mm level of accuracy and 16% (SD 0.3) of the trajectory for the 2 mm error.

As we considered our samples to be normally distributed due to the number of observations recorded (please refer to graph 2), we applied the two tailed test Student t-test, for paired data with different variance. The results of the Student t-test comparing the accuracy of AR-guided and surgical navigator-guided osteotomies are summarized as follows:

1. At a margin of error of 1.5 mm (assessed with cutting guides with the groove of 3 mm), the p-value obtained was 0.17. This p-value is greater than 0.05, indicating that there is no statistically significant difference in accuracy between the two methods at this margin of error. In this case, the AR-guided and surgical navigator-guided osteotomies showed comparable accuracy at a 1 mm margin of error.
2. At a margin of error of 1 mm (assessed with cutting guides of 2 mm), the p-value obtained was 0.001. This p-value is lower than the commonly used significance level of 0.05, indicating that there is statistically significant difference in accuracy between AR-guided and surgical navigator-guided osteotomies at this margin of error. In other words, the two methods performed differently in terms of accuracy when the margin of error was 1 mm.



**Graph 2:** this is the distribution of all the observations made by the three independent observers, with means, SD and median showed.

		Independent Samples Test										
		Levene's Test for Equality of Variances		t-test for Equality of Means							95% Confidence Interval of the Difference	
		F	Sig.	t	df	One-Sided p	Two-Sided p	Mean Difference	Std. Error Difference	Lower	Upper	
Measurement	Equal variances assumed	1.142	.286	-3.088	262	.001	.002	-13.962	4.521	-22.864	-5.060	
	Equal variances not assumed			-3.088	261.776	.001	.002	-13.962	4.521	-22.864	-5.060	

**Table 8:** t student for independent data AR vs NAV. In this case we considered both the determination for 1.5 mm and 1 mm accuracy levels as a whole data set.

We then performed a Student T test for independent data on the whole determinations of measurements of NAV vs AR, without distinguishing between 1.5- and 1-mm levels of accuracy (refer to table 8). We obtained a significant p value of 0.002, lower than the significance value. We rejected the null hypothesis, considering that there's a statistically significant difference between the accuracies of NAV and AR, with a d Cohen of 0.4 (medium effect size), and an average of 40% (DS 0.37) of the line traced under the guidance of the AR vs 26% (DS 0.36) obtained with NAV.

### 4.3. 1. Single Patient Analysis

Patients technical details are included in the following table.

Pt	Navigator	Tracking modality	Cutting Guides	Notes
1	NO	Model target	NO	
2	NO	Model target	YES	Non-specific shape
3	YES	Model target/Image Target	YES	
4	YES	Image Target	YES	
5	YES	Image Target	YES	Sterile Bag
6	YES	Image Target	YES	
7	No	Image Target	YES	CT scan older than 6 month prior to surgery
8	YES	Image Target	YES	Autotracking not working
9	YES	Image target	YES	Remote control
10	YES	Image target	YES	Remote control

**Table 9:** technical notes for each patient

In one case we did not introduce the comparison with the standard neurosurgical navigator, nor the accuracy cutting guides. In another case, we

had a problem with the cutting guides sterilization and we had to use them in a sterile bag, which made measurements more difficult.

We changed our method of tracking during the study, due to the difficulties encountered with the model target due to non-specific shapes (this was particularly evident with case n.2). In the last three cases with added the extra remote control to the normal one, to intervene, whether the operator had problems with the holographic toolbox. One case gave outlier results due to the fact that the CT scan was older than 6 months and the hologram did not fit the patient.

#### **4.4. Discussion**

AR on HMD can be a promising technology for surgery. This method is customized for each patient, providing dependable and comprehensive visualization, integrating virtual information (like the surgical planning) with the real environment. It enables natural and intuitive navigation, scalability, and the flexibility to manipulate and magnify the patient's image. Furthermore, it serves as a valuable instrument for fostering multidisciplinary deliberations and enhancing the efficiency of resources during preoperative surgical preparation [89].

AR holds significant potential in the medical field, particularly in surgery [5,14,23-29,81,82]. One of the major advantages of AR, when compared to the standard surgical navigator is eliminating the need for operators to shift their focus and allowing them to maintain concentration on the patient while holograms are projected onto the surgical field.

HMDs are commonly categorized into two primary types: optical see-through devices and video see-through devices [23-25, 27, 28, 79, 80-82]. In our investigation, we employed the optical see-through HoloLens 2 [5].

In craniofacial surgery, an HMD must offer high accuracy and maintain the integrity of holographic projections within the surgeon's field of view, even during movement. HoloLens has demonstrated its potential in addressing these requirements [13,25]. Nevertheless, certain limitations and challenges have been reported in the existing literature, including issues related to depth perception and registration errors [13, 27, 84]. Our previous experience has also identified some of these limitations [5, 13].

To tackle these challenges, our research group previously worked on mitigating registration errors, resulting in a static error range of 1 to 10 mm, which occasionally led to misalignment between virtual and actual images [84].

In our earlier study [13], we assessed the accuracy of HoloLens 2 in craniofacial surgery, with a particular focus on two osteotomies essential for fronto-orbital remodeling: the nasal and frontal osteotomies, which define the orbital bandeau. Six operators completed these tasks multiple times, with a one-week interval between trials to prevent a cumulative learning effect. The users traced the osteotomies using a pen under the guidance of HoloLens 2 projection, observing the phantom and dotted lines representing the planned osteotomies through their lenses. Some challenges related to virtual-to-real alignment and loss of sharpness were observed when moving the pen within the field of view.

Nevertheless, all users successfully completed the task. The osteotomies traced with the pen were subsequently verified using cutting guides with varying groove widths.

Our findings in terms of accuracy are consistent with prior literature and are, on the whole, encouraging, with the maximum reported error falling within  $\pm 1.5$  mm. In this current study, building upon the promising outcomes of our previous work, we included 8 patients and compared the osteotomy lines traced under the guidance of a surgical navigator with those traced using HoloLens 2. Our results demonstrated that HoloLens 2 performed well, with an error of 1.5 mm (accuracy level tested with the 3 mm cutting guide), and overall, they did not perform worse than the golden standard, the neurosurgical navigator. Our findings show that there's a difference between the two groups, especially when regarding the level of accuracy of 1 mm (assessed with the cutting guides with the groove of 2 mm), whereas the HoloLens2 seemed to perform better than the Neurosurgical Navigator, as we recorded a p value of 0.001, with the HoloLens accounting for an average of the 34% of the lines traced under their guidance vs the 16% traced under the guidance of the NAV. Empirically, we consider this results encouraging, but we are aware that this fluctuation might be due to the fact that with the standard navigator, the user had to turn his head continuously during the tracing of the line, while with HoloLens 2 they had the image continuously in front of them: this might have decreased the accuracy reported for the NAV. Nonetheless, these accuracy levels are in line with descriptions in existing literature [24, 25, 90, 91]. For instance, Scherl et al. reported accuracy of less than 1.3 mm in an in vivo study [25], while Tang et al. described a mean

deviation of  $1.68 \pm 0.92$  mm between preoperative virtual osteotomy planes and actual postoperative osteotomy planes in head and neck oncology [91]. We have also to highlight that the learning curve has been slightly more difficult in vivo, rather than our previous study [13], mostly because we were not under controlled, optimal experimental conditions.

Furthermore, our findings suggest that both methods are equally effective in guiding osteotomies within the specified margins of error, and in some cases HoloLens2 performed even better. However, it's crucial to consider the practical implications and limitations of the study when interpreting these results and their relevance to clinical practice.

# Chapter 5 **USERS' EXPERIENCE**

## 5.1 Users' experience

Alongside the major work on the feasibility of HoloLens 2 in craniofacial surgery, we have been administering an appreciation questionnaire to all the researchers involved in this study.

The main aim was to acknowledge if the technical results were accompanied with good evaluation of the ergonomics, usability and personal experience.

We have sent the questionnaire to 11 different researchers. Among those, 8 are surgeons and 3 engineers.

These were the questions:

### **Anagraphics**

Age

Gender

Institution

If Applicable, Surgical Specialty

Years of experience

### **Introductive questions**

Previous experience with AR (yes/no)

Usefulness of HoloLens2 for your surgery (1-5)

HoloLens2 make the work easier (1-5)

HoloLens 2 might improve the surgical result (1-5)

HoloLens 2 might reduce the surgical timing (1-5)

In which kind of operation, they could find the best application?

Would you introduce HoloLens2 in your current practice?

**Domain 1: usage of HoloLens 2**

The visualization of the model is good (1-5)

The tracking system is reliable (1-5)

The interaction with the 3D objects and hologram is easy (1-5)

I am satisfied with the wearability, comfort and ergonomics of the device (1-5)

The depth and the relations of the hologram with the real environment are good  
(1-5)

**Domain 2: applications of HoloLens 2**

Where would you apply the device? (Yes/No)

Diagnostics

Preoperative planning

In theatre for trainees

In theatre as a surgical guide

To explain the surgery to the patient

It was possible to answer the questions with open responses, and whenever indicated, by using YES/NO or the Likert scale from 1 to 5, whereas 1 stands for strongly disagree and 5 for completely agree. All the users found the questionnaire readable and easy to complete. The last domain had YES/NO questions.

## **5.2 Users' experience: results**

The most of the interviewed people are surgeons (8/11). We ranged from very experienced surgeons (over 10 years of experience, in 3 cases) to younger surgeons less than 10 years of experience (4/12) and also trainees (1).

Only 3 interviewees are engineers with a specialism in craniofacial surgery.

All the users had an overall positive attitude towards the device.

In the domains asking the interviewees to rate their experience with HoloLens, the mean answer was 3.35 +/- 0.67 SD.

In terms of applicability, 5 users out of 11 found that HoloLens might be useful in the diagnostic phase, whereas 10 of them think that HMDs will find their major application during the preoperative phase, in theatre during the procedure and to train the residents. Only 5 users found that HoloLens might be helpful for the patients to understand the surgery.

10 users think that HMDs will be introduced in the clinical practice, but all of them agree that improvements have to be made. The major application of the HoloLens2 might be in head and neck oncology, neurosurgical oncology and craniofacial surgery (see table 10). The overall impression has been satisfying, and the most of the interviewees agreed.

<b>Introductory questions</b>	<b>Median</b>	<b>IQR</b>
HoloLens2 make the work easier	3	0
HoloLens 2 might improve the surgical result	3	0
HoloLens 2 might reduce the surgical timing	3	1
<b>Domain 1: usage of HoloLens2</b>		
The visualization of the model is good	4	1
The tracking system is reliable	3	0
The interaction with the 3D objects and hologram is easy	3	1
I am satisfied with the wearability, comfort and ergonomics of the device	4	0
The depth and the relations of the hologram with the real environment are good	4	1

**Table 10:** these are a part of the users' answers, calculated with median, representing the central tendency of the answers, and IQR (inter-quartile rate) to assess the dispersion.

### 5.3 Discussion

Lately, there has been a comprehensive analysis published on the utilization of the first-generation HoloLens in the field of medicine, with it being identified as a significant driving force in medical augmented reality (AR) research in recent years [92]. 217 studies were included, from the release of the HoloLens in 2016 up to 2021. According to the review, the majority of research efforts are centered on aiding surgeons during medical procedures. Nevertheless, it is widely agreed that the accuracy and reliability of these systems are still insufficient to replace traditional guidance systems, despite our Group has been recently demonstrating that they might be comparable. On the other hand, the second most commonly targeted use is in AR-enhanced medical simulation platforms. In this context, the HoloLens has shown promise due to its capacity

to enhance the perception and comprehension of human anatomy during pre-intervention planning and learning phases. Our users agreed with the major employability of the HoloLens during the preoperative phase, the intervention and for training purposes. Other studies have been advocating the advantages in a navigation obtained by means of HMD, as a valuable asset in neurosurgery [93].

However, we are still far from claiming that HMD can substitute the standard neurosurgical navigation. Some studies privilege and advocate their usage in low-risk scenario like surgical simulation or surgical supervision [13, 94]

Some studies have been also comparing different kind of HMDs, highlighting their potentials in both the preoperative planning and the simulation for trainees [95], preferring Magic Leap by Google, whereas other Authors found that AR in surgical education is both feasible and effective as a complement to conventional training, with the Microsoft HoloLens exhibiting the most promising outcomes across all aspects and enhancing the performance of surgical trainees [96].

Our experience has been overall extremely positive, and the majority of the users would include HoloLens in their practice, with certain ameliorations.

# Chapter 6 **CONCLUSIONS**

## **6.1 Conclusions**

AR has demonstrated to be a promising technology in the medical field. The growing fortune that it has been achieving in the surgical field in the last years, is a sign that it might be soon incorporated in the usual practice.

Our group experience has been overall positive. From the tests on phantom to the application on real patients, the users' had an encouraging experience, and we are now implementing the usage of AR on HMDs in our clinical practice.

We recognize that one of our major limitations is the small number of patients enrolled, but further research is already ongoing to corroborate our data.

## REFERENCES

1. Smith, A. B., & Jones, C. M. (Eds.). (2020). \*Craniofacial Surgery.\* Springer
2. Johnson, E. F., & Paredes, J. L. (2018). Augmented reality in surgery: The digital surgical environment. In \*Advances in computer and information sciences and engineering\* (pp. 195-208). Springer.
3. Microsoft. (2021). \*HoloLens 2.\* <https://www.microsoft.com/en-us/hololens>
4. Cutolo, F., Meola, A., & Carbone, M. (2017). The Role of Augmented Reality in Surgery: Review. In \*Smart Innovation, Systems and Technologies\* (Vol. 67, pp. 273-280). Springer
5. Ayoub A, Pulijala Y The application of virtual reality and augmented reality in Oral & Maxillofacial Surgery BMC Oral Health 19:238 (2019)
6. R Azuma. "A survey of augmented reality presence". In: *Teleoperators and Virtual Environments* 6.4 (1997), pp. 355–385. ISSN: 10547460.
7. T Sielhorst, M Feuerstein, and N Navab. "Advanced medical displays: A literature review of augmented reality". In: *Journal of Display Technology* 4.4 (2008), pp. 451–467
8. Badiali G, Cutolo F, Cercenelli L, Carbone M, D'Amato R, Ferrari V, et al. The Vostars Project: A New Wearable Hybrid Video and Optical See-Through Augmented

Reality Surgical System for Maxillofacial Surgery. *Int J Oral Maxillofac Surg* (2019) 48:153. doi: 10.1016/j.ijom.2019.03.472

9. Cercenelli L, Carbone M, Condino S, Cutolo F, Marcelli E, Tarsitano A, et al. The Wearable VOSTARS System for Augmented Reality-Guided Surgery: Preclinical Phantom Evaluation for High-Precision Maxillofacial Tasks. *J Clin Med* (2020) 9(11):E3562. doi: 10.3390/jcm9113562

10. P Holland and H Fuchs. "Optical versus Video See-Through Head-Mounted Displays". In: *Fundamentals of Wearable Computers and Augmented Reality* (2001), p. 113.

11. Zari G, Condino S, Cutolo F, Ferrari V. Magic Leap 1 versus Microsoft HoloLens 2 for the Visualization of 3D Content Obtained from Radiological Images. *Sensors*. 2023; 23(6):3040. <https://doi.org/10.3390/s23063040>

12. P Milgram, H Takemura, a Utsumi, and F Kishino. "Mixed Reality ( MR ) Reality-Virtuality ( RV ) Continuum". In: *Systems Research 2351. Telemanipulator and Telepresence Technologies* (1994), pp. 282–292.

13. Ruggiero F, Cercenelli L, Emiliani N, Badiali G, Bevini M, Zucchelli M, Marcelli E, Tarsitano A. Preclinical Application of Augmented Reality in Pediatric Craniofacial Surgery: An Accuracy Study. *J Clin Med*. 2023 Apr 4;12(7):2693. doi: 10.3390/jcm12072693

14. Marzano, E. et al. Augmented reality-guided artery-first pancreaticoduodenectomy. *Journal of gastrointestinal surgery: official journal of the Society for Surgery of the Alimentary Tract* **17**, 1980–1983, <https://doi.org/10.1007/s11605-013-2307-1> (2013)
15. Ghaednia H, Fourman MS, Lans A, Detels K, Dijkstra H, Lloyd S, Sweeney A, Oosterhoff JHF, Schwab JH. Augmented and virtual reality in spine surgery, current applications and future potentials. *Spine J.* 2021 Oct;21(10):1617-1625. doi: 10.1016/j.spinee.2021.03.018. Epub 2021 Mar 25.
- 16 Verhey JT, Haglin JM, Verhey EM, Hartigan DE. “Virtual, augmented, and mixed reality applications in orthopedic surgery”. *Int J Med Robot.* 2020 Apr;16(2):e2067. doi: 10.1002/rcs.2067. Epub 2020 Feb 6.
- 17 Quero G, Lapergola A, Soler L, Shahbaz M, Hostettler A, Collins T, Marescaux J, Mutter D, Diana M, Pessaux P. “Virtual and Augmented Reality in Oncologic Liver Surgery”. *Surg Oncol Clin N Am.* 2019 Jan;28(1):31-44. doi: 10.1016/j.soc.2018.08.002.
- 18 Aguilar-Salinas P, Gutierrez-Aguirre SF, Avila MJ, Nakaji P. Current status of augmented reality in cerebrovascular surgery: a systematic review. *Neurosurg Rev.* 2022 Jun;45(3):1951-1964.
- 19 R. Schiavina, L. Bianchi, S. Lodi, L. Cercenelli, F. Chessa, B. Bortolani, C. Gaudiano, C. Casablanca, M. Droghetti, A. Porreca, D. Romagnoli, R. Golfieri, F. Giunchi, M. Fiorentino, E. Marcelli, S. Diciotti, E. Brunocilla. “Real-time Augmented

Reality Three-dimensional Guided Robotic Radical Prostatectomy: Preliminary Experience and Evaluation of the Impact on Surgical Planning”. Eur Urol Focus 2021 Nov;7(6):1260-1267.doi: 10.1016/j.euf.2020.08.004. Epub 2020 Sep 1. doi: 10.1016/j.euf.2020.08.004.

20 R. Schiavina, L. Bianchi, F. Chessa, U. Barbaresi, L. Cercenelli, S. Lodi, C. Gaudiano, B. Bortolani, A. Angiolini, F. Mineo Bianchi, A. Ercolino, C. Casablanca, E. Molinaroli, A.Porreca, R. Golfieri, S. Diciotti, E. Marcelli, E. Brunocilla. “Augmented Reality to Guide Selective Clamping and Tumor Dissection During Robot-assisted Partial Nephrectomy: A Preliminary Experience”. Clin Genitourin Cancer 2021 Jun;19(3):e149-e155. doi: 10.1016/j.clgc.2020.09.005. Epub 2020 Sep 18.

21 L. Bianchi, F. Chessa, A. Angiolini, L. Cercenelli, S. Lodi, B. Bortolani, E. Molinaroli, C.Casablanca, M. Droghetti, C. Gaudiano, A. Mottaran, A.Porreca, R. Golfieri, D. Romagnoli, F. Giunchi, M. Fiorentino, P.Piazza, S. Puliatti, S. Diciotti, E. Marcelli, A. Mottrie, R. Schiavina. “The Use of Augmented Reality to Guide the Intraoperative Frozen Section During Robot-assisted Radical Prostatectomy”. Eur Urol 2021 Oct;80(4):480-488.doi: 10.1016/j.eururo.2021.06.020. Epub 2021 Jul 29

22 Kim Y, Kim H, Kim YO. Virtual reality and augmented reality in plastic surgery: a review. Arch Plast Surg.;44(3):179–87 (2017)

- 23 Okamoto, T., Onda, S., Yanaga, K., Suzuki, N. & Hattori, A. Clinical application of navigation surgery using augmented reality in the abdominal field. *Surgery today* **45**, 397–406 (2015)
- 24 Scherl C, Stratemeier J, Rotter N, Hesser J, Schönberg SO, Servais JJ, Männle D, Lammert A. Augmented Reality with HoloLens® in Parotid Tumor Surgery: A Prospective Feasibility Study. *ORL J Otorhinolaryngol Relat Spec.* 2021;83(6):439-448. doi: 10.1159/000514640.
- 25 Scherl C, Stratemeier J, Karle C, Rotter N, Hesser J, Huber L, Dias A, Hoffmann O, Riffel P, Schoenberg SO, Schell A, Lammert A, Affolter A, Männle D. Augmented reality with HoloLens in parotid surgery: how to assess and to improve accuracy. *Eur Arch Otorhinolaryngol.* 2021 Jul;278(7):2473-2483. doi: 10.1007/s00405-020-06351-7
- 26 Guha D, Alotaibi NM, Nguyen N, Gupta S, McFaul C, Yang VXD. Augmented Reality in Neurosurgery: A Review of Current Concepts and Emerging Applications. *Can J Neurol Sci.* 2017 May;44(3):235-245. doi: 10.1017/cjn.2016.443. Epub 2017 Apr 24. PMID: 28434425.
- 27 Badiali, G. et al. Augmented reality as an aid in maxillofacial surgery: validation of a wearable system allowing maxillary repositioning. *Journal of cranio-maxillo-facial surgery: official publication of the European Association for Cranio-Maxillo-Facial Surgery* **42**, 1970–1976, <https://doi.org/10.1016/j.jcms.2014.09.001> (2014).

- 28 Qu M, Hou Y, Xu Y, Shen C, Zhu M, Xie L, Wang H, Zhang Y, Chai G. Precise positioning of an intraoral distractor using augmented reality in patients with hemifacial microsomia. *J Craniomaxillofac Surg*. 2015 Jan;43(1):106-12. doi: 10.1016/j.jcms.2014.10.019.
- 29 Ceccariglia F, Cercenelli L, Badiali G, Marcelli E, Tarsitano A. Application of Augmented Reality to Maxillary Resections: A Three-Dimensional Approach to Maxillofacial Oncologic Surgery. *J Pers Med*. 2022 Dec 12;12(12):2047. doi: 10.3390/jpm12122047
- 30 Guo F, Wang J, Li Y, et al. *Mixed reality technology in medical education: a literature review. Medicine (Baltimore)*. 2020;99(24):e20347.
- 31 Marescaux J, Diana M. *Next-generation surgical platforms: a challenge to the next generation of surgeons. Ann Surg*. 2019;269(1):10-12.
- 32 Ponce BA, Jennings JK, Clay TB, et al. *Telementoring: Use of augmented reality in orthopaedic education: AAOS exhibit selection. J Bone Joint Surg Am*. 2014;96(10):e84.
- 33 Lobo D, Lanciego C, Feito FR, et al. *Usefulness of mixed reality for patient education of a child with epilepsy: A case report. Pediatr Neurol*. 2020;104:73-75.
- 34 Khanna PC, Thapa MM, Iyer RS, Prasad SS (January 2011). ["Pictorial essay: The many faces of craniosynostosis"](#). *The Indian Journal of Radiology &*

- Imaging.* **21** (1): 49–56. [doi:10.4103/0971-3026.76055](https://doi.org/10.4103/0971-3026.76055). [PMC 3056371](https://pubmed.ncbi.nlm.nih.gov/3056371/). [PMID 21431034](https://pubmed.ncbi.nlm.nih.gov/21431034/).
- 35 Silva S, Jeanty P (1999-06-07). "[Cloverleaf skull or kleeblattschadel](#)". *TheFetus.net. MacroMedia*. Archived from [the original](#) on 2007-01-07. Retrieved 2007-02-03
- 36 Moss ML: Functional anatomy of cranial synostosis. *Childs Brain* 1:22–33 (1975).
- 37 Slater BJ, Lenton KA, Kwan MD, Gupta DM, Wan DC, Longaker MT (April 2008). "Cranial sutures: a brief review". *Plastic and Reconstructive Surgery.* **121** (4): 170e–8e. [doi:10.1097/01.prs.0000304441.99483.97](https://doi.org/10.1097/01.prs.0000304441.99483.97). [PMID 18349596](https://pubmed.ncbi.nlm.nih.gov/18349596/). [S2CID 34344899](https://pubmed.ncbi.nlm.nih.gov/34344899/).
- 38 Gault DT, Renier D, Marchac D, Jones BM (September 1992). "Intracranial pressure and intracranial volume in children with craniosynostosis". *Plastic and Reconstructive Surgery.* **90** (3): 377–81. [doi:10.1097/00006534-199209000-00003](https://doi.org/10.1097/00006534-199209000-00003). [PMID 1513883](https://pubmed.ncbi.nlm.nih.gov/1513883/).
- 39 Bannink N, Nout E, Wolvius EB, Hoeve HL, Joosten KF, Mathijssen IM (February 2010). "Obstructive sleep apnea in children with syndromic craniosynostosis: long-term respiratory outcome of midface advancement". *International Journal of Oral and Maxillofacial Surgery.* **39**(2): 115–21. [doi:10.1016/j.ijom.2009.11.021](https://doi.org/10.1016/j.ijom.2009.11.021). [PMID 20056390](https://pubmed.ncbi.nlm.nih.gov/20056390/).
- 40 van der Meulen J. Metopic synostosis. *Childs Nerv Syst.* 2012 Sep;28(9):1359-67. doi: 10.1007/s00381-012-1803-z. Epub 2012 Aug 8. PMID: 22872249; PMCID: PMC3413823.
- 41 van der Meulen J, van der Hulst R, van Adrichem L, Arnaud E, Chin-Shong D, Duncan C, Habets E, Hinojosa J, Mathijssen I, May P, Morritt D, Nishikawa H,

Noons P, Richardson D, Wall S, van der Vlugt J, Renier D. The increase of metopic synostosis: a pan-European observation. *J Craniofac Surg*. 2009 Mar;20(2):283-6. doi: 10.1097/scs.0b013e31818436be. PMID: 19326483.

42 Mathijssen IMJ; Working Group Guideline Craniosynostosis. Updated Guideline on Treatment and Management of Craniosynostosis. *J Craniofac Surg*. 2021 Jan-Feb 01;32(1):371-450. doi: 10.1097/SCS.00000000000007035

43 Lattanzi W, Barba M, Di Pietro L, Boyadjiev SA. Genetic advances in craniosynostosis. *Am J Med Genet A*. 2017 May;173(5):1406-1429. doi: 10.1002/ajmg.a.38159. Epub 2017 Feb 4. PMID: 28160402; PMCID: PMC5397362.

44 Greenwood J, Flodman P, Osann K, Boyadjiev SA, Kimonis V. Familial incidence and associated symptoms in a population of individuals with nonsyndromic craniosynostosis. *Genet Med*. 2014 Apr;16(4):302-10. doi: 10.1038/gim.2013.134. Epub 2013 Sep 26. PMID: 24071792; PMCID: PMC4143991.

45 Lajeunie E, Crimmins DW, Arnaud E, Renier D. Genetic considerations in nonsyndromic midline craniosynostoses: a study of twins and their families. *J Neurosurg*. 2005 Oct;103(4 Suppl):353-6. doi: 10.3171/ped.2005.103.4.0353. PMID: 16270687.

- 46 Birgfeld CB, Saltzman BS, Hing AV, Heike CL, Khanna PC, Gruss JS, Hopper RA. Making the diagnosis: metopic ridge versus metopic craniosynostosis. *J Craniofac Surg.* 2013 Jan;24(1):178-85. doi: 10.1097/SCS.0b013e31826683d1. PMID: 23348281.
- 47 Kelleher MO, Murray DJ, McGillivray A, Kamel MH, Allcutt D, Earley MJ. Behavioral, developmental, and educational problems in children with nonsyndromic trigonocephaly. *J Neurosurg.* 2006 Nov;105(5 Suppl):382-4. doi: 10.3171/ped.2006.105.5.382. PMID: 17328262.
- 48 Aryan HE, Jandial R, Ozgur BM, Hughes SA, Meltzer HS, Park MS, Levy ML. Surgical correction of metopic synostosis. *Childs Nerv Syst.* 2005 May;21(5):392-8. doi: 10.1007/s00381-004-1108-y. Epub 2005 Feb 16. PMID: 15714353.
- 49 Sidoti EJ Jr, Marsh JL, Marty-Grames L, Noetzel MJ. Long-term studies of metopic synostosis: frequency of cognitive impairment and behavioral disturbances. *Plast Reconstr Surg.* 1996 Feb;97(2):276-81. doi: 10.1097/00006534-199602000-00002. PMID: 8559809.
- 50 Lajeunie E, Le Merrer M, Marchac D, Renier D. Syndromal and nonsyndromal primary trigonocephaly: analysis of a series of 237 patients. *Am J Med Genet.* 1998 Jan 13;75(2):211-5. doi: 10.1002/(sici)1096-8628(19980113)75:2<211::aid-ajmg19>3.0.co;2-s. PMID: 9450889.

- 51 van der Vlugt JJB, van der Meulen JJNM, Creemers HE, Verhulst FC, Hovius SER, Okkerse JME. Cognitive and behavioral functioning in 82 patients with trigonocephaly. *Plast Reconstr Surg*. 2012 Oct;130(4):885-893. doi: 10.1097/PRS.0b013e318262f21f. PMID: 23018698.
- 52 Kapp-Simon KA, Leroux B, Cunningham M, Speltz ML. Multisite study of infants with single-suture craniosynostosis: preliminary report of presurgery development. *Cleft Palate Craniofac J*. 2005 Jul;42(4):377-84. doi: 10.1597/04-044.1. PMID: 16001919.
- 53 Speltz ML, Kapp-Simon K, Collett B, Keich Y, Gaither R, Craddock MM, Buono L, Cunningham ML. Neurodevelopment of infants with single-suture craniosynostosis: presurgery comparisons with case-matched controls. *Plast Reconstr Surg*. 2007 May;119(6):1874-1881. doi: 10.1097/01.prs.0000259184.88265.3f. PMID: 17440368; PMCID: PMC3417765.
- 54 Starr JR, Kapp-Simon KA, Cloonan YK, Collett BR, Craddock MM, Buono L, Cunningham ML, Speltz ML. Presurgical and postsurgical assessment of the neurodevelopment of infants with single-suture craniosynostosis: comparison with controls. *J Neurosurg*. 2007 Aug;107(2 Suppl):103-10. doi: 10.3171/PED-07/08/103. PMID: 18459881; PMCID: PMC3417768.
- 55 Mathijssen IM. Guideline for Care of Patients With the Diagnoses of Craniosynostosis: Working Group on Craniosynostosis. *J Craniofac Surg*. 2015 Sep;26(6):1735-807. doi: 10.1097/SCS.0000000000002016. PMID: 26355968; PMCID: PMC4568904.

- 56 Kapp-Simon KA, Speltz ML, Cunningham ML, Patel PK, Tomita T (March 2007). "Neurodevelopment of children with single suture craniosynostosis: a review". *Child's Nervous System*. **23** (3): 269–81. [doi:10.1007/s00381-006-0251-z](https://doi.org/10.1007/s00381-006-0251-z). [PMID 17186250](https://pubmed.ncbi.nlm.nih.gov/17186250/). [S2CID 29722887](https://pubmed.ncbi.nlm.nih.gov/29722887/).
- 57 Cunningham ML, Heike CL (December 2007). "Evaluation of the infant with an abnormal skull shape". *Current Opinion in Pediatrics*. **19** (6): 645–51. [doi:10.1097/MOP.0b013e3282f1581a](https://doi.org/10.1097/MOP.0b013e3282f1581a). [PMID 18025930](https://pubmed.ncbi.nlm.nih.gov/18025930/). [S2CID 26966396](https://pubmed.ncbi.nlm.nih.gov/26966396/)
- 58 Levy, Richard Lawrence; Rogers, Gary F.; Mulliken, John B.; Proctor, Mark R.; Dagi, Linda R. (2007). "Astigmatism in unilateral coronal synostosis: Incidence and laterality". *J AAPOS*. **11** (4): 367–372. [doi:10.1016/j.jaapos.2007.02.017](https://doi.org/10.1016/j.jaapos.2007.02.017). [PMID 17588790](https://pubmed.ncbi.nlm.nih.gov/17588790/).
- 59 Huang MH, Gruss JS, Clarren SK, Mouradian WE, Cunningham ML, Roberts TS, Loeser JD, Cornell CJ (October 1996). "The differential diagnosis of posterior plagiocephaly: true lambdoid synostosis versus positional molding". *Plastic and Reconstructive Surgery*. **98** (5): 765–74, discussion 775–6. [doi:10.1097/00006534-199610000-00002](https://doi.org/10.1097/00006534-199610000-00002). [PMID 8823012](https://pubmed.ncbi.nlm.nih.gov/8823012/).
- 60 Persing JA (April 2008). "MOC-PS(SM) CME article: management considerations in the treatment of craniosynostosis". *Plastic and Reconstructive Surgery*. **121** (4 Suppl): 1–11. [doi:10.1097/01.prs.0000305929.40363.bf](https://doi.org/10.1097/01.prs.0000305929.40363.bf). [PMID 18379381](https://pubmed.ncbi.nlm.nih.gov/18379381/).

- 61 Chumas PD, Cinalli G, Arnaud E, Marchac D, Renier D (February 1997). "Classification of previously unclassified cases of craniosynostosis". *Journal of Neurosurgery*. **86** (2): 177–81. [doi:10.3171/jns.1997.86.2.0177](https://doi.org/10.3171/jns.1997.86.2.0177). [PMID 9010415](https://pubmed.ncbi.nlm.nih.gov/9010415/).
- 62 Blount JP, Louis RG, Tubbs RS, Grant JH (October 2007). "Pansynostosis: a review". *Child's Nervous System*. **23** (10): 1103–9. [doi:10.1007/s00381-007-0362-1](https://doi.org/10.1007/s00381-007-0362-1). [PMID 17486351](https://pubmed.ncbi.nlm.nih.gov/17486351/). [S2CID 43068552](https://pubmed.ncbi.nlm.nih.gov/43068552/).
- 63 Cohen MM Jr: Craniofrontonasal dysplasia. *Birth Defects Orig Artic Ser* 15:85–89 (1979).
- 64 Robin NH, Falk MJ, Haldeman-Englert CR: *FGFR*-related craniosynostosis syndromes, in Adam MP, Ardinger HH, Pagon RA, Wallace SE, Bean LJH, et al (eds): GeneReviews® [Internet] (University of Washington, Seattle (WA): Seattle 1993–2018). Initial posting: Oct 20, 1998; last update: June 7, 2011.
- 65 Forrest CR, Hopper RA: Craniofacial syndromes and surgery. *Plast Reconstr Surg* 131:86e– 109e (2013).
- 66 Britto JA, Chan JC, Evans RD, Hayward RD, Jones BM: Differential expression of fibroblast growth factor receptors in human digital development suggests common pathogenesis in complex acrosyndactyly and craniosynostosis. *Plast Reconstr Surg* 107:1331–1338 (2001).
- 67 Rice DP: Clinical features of syndromic craniosynostosis. *Front Oral Biol* 12:91–106 (2008).

- 68 Johnson D, Wilkie AO: Craniosynostosis. *Eur J Hum Genet* 19:369–376 (2011).
- 69 Cho E, Yang TH, Shin ES, Byeon JH, Kim GH, Eun BL: Saethre–Chotzen syndrome with an atypical phenotype: identification of *TWIST* microdeletion by array CGH. *Childs Nerv Syst* 29:2101–2104 (2013).
- 70 O'Hara J, Ruggiero F, Wilson L, James G, Glass G, Jeelani O, Ong J, Bowman R, Wyatt M, Evans R, Samuels M, Hayward R, Dunaway DJ. Syndromic Craniosynostosis: Complexities of Clinical Care. *Mol Syndromol*. 2019 Feb;10(1-2):83-97. doi: 10.1159/000495739
- 71 Rodriguez-Florez N, Göktekin ÖK, Bruse JL, Borghi A, Angullia F, Knoops PG, Tenhagen M, O'Hara JL, Koudstaal MJ, Schievano S, Jeelani NU, James G, Dunaway DJ. Quantifying the effect of corrective surgery for trigonocephaly: A non-invasive, non-ionizing method using three-dimensional handheld scanning and statistical shape modelling. *J Craniomaxillofac Surg*. 2017 Mar;45(3):387-394. doi: 10.1016/j.jcms.2017.01.002. Epub 2017 Jan 10. PMID: 28159480.
- 72 Friede H, Alberius P, Lilja J, Lauritzen C. Trigonocephaly: clinical and cephalometric assessment of craniofacial morphology in operated and nontreated patients. *Cleft Palate J*. 1990 Oct;27(4):362-7; discussion 368. doi: 10.1597/1545-1569(1990)027<0362:tcacao>2.3.co;2. PMID: 2253382.
- 73 Selber J, Reid RR, Gershman B, Sonnad SS, Sutton LN, Whitaker LA, Bartlett SP. Evolution of operative techniques for the treatment of single-suture metopic

synostosis. *Ann Plast Surg.* 2007 Jul;59(1):6-13. doi:

10.1097/01.sap.0000264836.54760.32. PMID: 17589251.

74 van der Meulen JJ, Nazir PR, Mathijssen IM, van Adrichem LN, Ongkosuwito E, Stolk-Liefferink SA, Vaandrager MJ. Bitemporal depressions after cranioplasty for trigonocephaly: a long-term evaluation of (supra) orbital growth in 92 patients. *J Craniofac Surg.* 2008 Jan;19(1):72-9. doi: 10.1097/scs.0b013e31815c8a68. PMID: 18216668.

75 Renier D, Lajeunie E, Arnaud E, Marchac D. Management of craniosynostoses. *Childs Nerv Syst.* 2000 Nov;16(10-11):645-58. doi: 10.1007/s003810000320. PMID: 11151714.

76 Ezaldein HH, Metzler P, Persing JA, Steinbacher DM. Three-dimensional orbital dysmorphology in metopic synostosis. *J Plast Reconstr Aesthet Surg.* 2014 Jul;67(7):900-5. doi: 10.1016/j.bjps.2014.03.009. Epub 2014 Apr 13. PMID: 24820454.

77 Posnick JC, Lin KY, Chen P, Armstrong D. Metopic synostosis: quantitative assessment of presenting deformity and surgical results based on CT scans. *Plast Reconstr Surg.* 1994 Jan;93(1):16-24. PMID: 8278471.

78 Fearon JA, Ruotolo RA, Kolar JC. Single sutural craniosynostoses: surgical outcomes and long-term growth. *Plast Reconstr Surg.* 2009 Feb;123(2):635-642. doi: 10.1097/PRS.0b013e318195661a. PMID: 19182624.

- 79 Cercenelli L, Babini F, Badiali G, Battaglia S, Tarsitano A, Marchetti C, Marcelli E. Augmented Reality to Assist Skin Paddle Harvesting in Osteomyocutaneous Fibular Flap Reconstructive Surgery: A Pilot Evaluation on a 3D-Printed Leg Phantom. *Front Oncol.* 2022 Jan 6;11:804748. doi: 10.3389/fonc.2021.804748.
- 80 Porpiglia F, Fiori C, Checcucci E, Amparore D, Bertolo R (2018) Augmented reality robot-assisted radical prostatectomy: preliminary experience. *Urology* 115:184. <https://doi.org/10.1016/j.urology.2018.01.028>
- 81 Elmi-Terander A, Nachabe R, Skulason H, Pedersen K, Söderman M, Racadio J, Babic D, Gerdhem P, Edström E (2018) Feasibility and accuracy of thoracolumbar minimally invasive pedicle screw placement with augmented reality navigation technology. *Spine (Phila Pa)* 43(14):1018–1023. <https://doi.org/10.1097/brs.0000000000002502>
- 82 Bong JH, Song HJ, Oh Y, Park N, Kim H, Park S (2018) Endoscopic navigation system with extended field of view using augmented reality technology. *Int J Med Robot.* <https://doi.org/10.1002/rcs.1886>
- 83 Qian L, Barthel A, Johnson A, Osgood G, Kazanzides P, Navab N, Fuerst B (2017) Comparison of optical see-through head-mounted displays for surgical interventions with object-anchored 2D-display. *Int J CARS* 12:901–910. <https://doi.org/10.1007/s11548-017-1564-y>

- 84 Badiali, G.; Cercenelli, L.; Battaglia, S.; Marcelli, E.; Marchetti, C.; Ferrari, V.; Cutolo, F. Review on Augmented Reality in Oral and Cranio-Maxillofacial Surgery: Toward“Surgery-Specific” Head-Up Displays. **2020**, IEEE Access 2020, 59015–59028, doi:10.1109/ACCESS.2020.2973298.
- 85 van Doormaal TPC, van Doormaal JAM, Mensink T. Clinical Accuracy of Holographic Navigation Using Point-Based Registration on Augmented-Reality Glasses. *Oper Neurosurg (Hagerstown)*. 2019 Dec 1;17(6):588-593. doi: 10.1093/ons/opz094.
- 86 Tang ZN, Hu LH, Soh HY, Yu Y, Zhang WB, Peng X. Accuracy of Mixed Reality Combined With Surgical Navigation Assisted Oral and Maxillofacial Tumor Resection. *Front Oncol*. 2022 Jan 14;11:715484. doi:10.3389/fonc.2021.715484.
- 87 Han W, Yang X, Wu S, Fan S, Chen X, Aung ZM, Liu T, Zhang Y, Gu S, Chai G. A new method for cranial vault reconstruction: Augmented reality in synostotic plagiocephaly surgery. *J Craniomaxillofac Surg*. 2019 Aug;47(8):1280-1284. doi: 10.1016/j.jcms.2019.04.008.
- 88 Cercenelli L, Carbone M, Condino S, Cutolo F, Marcelli E, Tarsitano A, et al. The Wearable VOSTARS System for Augmented Reality-Guided Surgery: Preclinical Phantom Evaluation for High-Precision Maxillofacial Tasks. *J Clin Med (2020)* 9(11):E3562. doi: 10.3390/jcm9113562
- 89 Coelho G, Rabelo NN, Vieira E, Mendes K, Zagatto G, Santos de Oliveira R, Raposo-Amaral CE, Yoshida M, de Souza MR, Fagundes CF, Teixeira MJ, Figueiredo EG. Augmented reality and physical hybrid model simulation for

- preoperative planning of metopic craniosynostosis surgery. *Neurosurg Focus*. 2020 Mar 1;48(3):E19. doi: 10.3171/2019.12.FOCUS19854.
- 90 van Doormaal TPC, van Doormaal JAM, Mensink T. Clinical Accuracy of Holographic Navigation Using Point-Based Registration on Augmented-Reality Glasses. *Oper Neurosurg (Hagerstown)*. 2019 Dec 1;17(6):588-593. doi: 10.1093/ons/opz094.
- 91 Tang ZN, Hu LH, Soh HY, Yu Y, Zhang WB, Peng X. Accuracy of Mixed Reality Combined With Surgical Navigation Assisted Oral and Maxillofacial Tumor Resection. *Front Oncol*. 2022 Jan 14;11:715484. doi:10.3389/fonc.2021.715484.
- 92 Gsaxner, C.; Li, J.; Pepe, A.; Jin, Y.; Kleesiek, J.; Schmalstieg, D.; Egger, J. The HoloLens in medicine: A systematic review and taxonomy. *Med. Image Anal.* 2023, 85, 102757.
- 93 Cho, J.; Rahimpour, S.; Cutler, A.; Goodwin, C.R.; Lad, S.P.; Codd, P. Enhancing Reality: A Systematic Review of Augmented Reality in Neuronavigation and Education. *World Neurosurg*. 2020
- 94 Rai, A.T.; Deib, G.; Smith, D.; Boo, S. Teleproctoring for Neurovascular Procedures: Demonstration of Concept Using Optical See-Through Head-Mounted Display, Interactive Mixed Reality, and Virtual Space Sharing-A Critical Need Highlighted by the COVID-19 Pandemic. *Am. J. Neuroradiol.* **2021**

95 Zari G, Condino S, Cutolo F, Ferrari V. Magic Leap 1 versus Microsoft HoloLens 2 for the Visualization of 3D Content Obtained from Radiological Images. *Sensors*. 2023; 23(6):3040. <https://doi.org/10.3390/s23063040>

96 Suresh D, Aydin A, James S, Ahmed K, Dasgupta P. The Role of Augmented Reality in Surgical Training: A Systematic Review. *Surg Innov*. 2023 Jun;30(3):366-382. doi: 10.1177/15533506221140506.

